



W&M ScholarWorks

Undergraduate Honors Theses

Theses, Dissertations, & Master Projects

5-2011

Evaluation of Micro-Preconcentrators and Solid Phase Microextraction Fibers for MEMS-based Gas Chromatography Systems

Ashley Marie Hoover
College of William and Mary

Follow this and additional works at: <https://scholarworks.wm.edu/honorstheses>

Recommended Citation

Hoover, Ashley Marie, "Evaluation of Micro-Preconcentrators and Solid Phase Microextraction Fibers for MEMS-based Gas Chromatography Systems" (2011). *Undergraduate Honors Theses*. Paper 431.
<https://scholarworks.wm.edu/honorstheses/431>

This Honors Thesis is brought to you for free and open access by the Theses, Dissertations, & Master Projects at W&M ScholarWorks. It has been accepted for inclusion in Undergraduate Honors Theses by an authorized administrator of W&M ScholarWorks. For more information, please contact scholarworks@wm.edu.

**Evaluation of Micro-Preconcentrators and Solid Phase Microextraction Fibers for
MEMS-based Gas Chromatography Systems**

A thesis submitted in partial fulfillment of the requirement
for the degree of Bachelor of Science in Chemistry from
The College of William and Mary

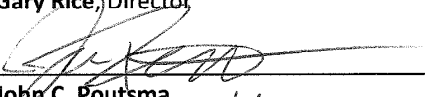
by

Ashley Marie Hoover

Accepted for Honors



Dr. Gary Rice, Director



Dr. John C. Poutsma



Dr. Irina Novikova

Williamsburg, VA
May 4, 2011

Table of Contents

Acknowledgements.....	v
List of Figures.....	vi
List of Tables.....	viii
Abstract.....	ix
I. Introduction and Background.....	1
Gas Chromatography as an Analytical Tool.....	1
Analysis of Volatile Organic Compounds.....	3
Microelectromechanical Systems Based Micro-GCs.....	4
Preconcentration.....	5
MEMS-Fabricated Micropreconcentrators.....	7
Solid-Phase Microextraction.....	11
Tenax.....	13
Purpose.....	14
II. Experimental Parameters and Procedures.....	15
MEMS-based Micro-Preconcentrator Design and Fabrication.....	15
Experimental Instrumentation for MEMS Preconcentrator Tests.....	21
Adsorption/Desorption Testing Setup.....	21
GC Flow Calibration for Preconcentrator Testing Setup.....	22
Blank Preconcentrator Heating.....	22
Reagent Preparation for Preconcentrator Experiments.....	23
Preconcentration of VOCs (Adsorption/Thermal Desorption).....	25

Timed Adsorption/Desorption with MEMS Preconcentrators.....	26
Preconcentrator-to-Column Coupling.....	26
Solid Phase Micro-Extraction (SPME) Fiber Coating.....	29
SPME Fiber Holder.....	30
SPME Reagent Preparation.....	30
Experimental Instrumentation for SPME Fiber Tests.....	32
Standard GC-MS Runs.....	33
Thermal Fiber Cleansing.....	33
Headspace Analysis.....	34
III. Results and Discussion: MEMS Preconcentrators.....	35
MEMS Preconcentrators Tested.....	35
Preconcentrator #2.....	35
Preconcentrator #5.....	41
Preconcentrator #6.....	46
Preconcentrator #8.....	50
Preconcentrator #9.....	54
Preconcentrator #11.....	58
Preconcentrator #R100.....	64
Preconcentrator #R200.....	66
Comparison of Preconcentrators	67
Preconcentrator-to-Column Coupling Experiment.....	69

IV. Results and Discussion: Preliminary SPME Evaluation.....	71
Ten-Component VOC Mix Standard Runs on the GC-MS.....	71
SPME Fiber Headspace Analysis of Spiked Water.....	71
V. Conclusions and Future Work.....	73
VI. References.....	77

In Memory of Poly Styrene of the X-Ray Spex

Acknowledgements

I would like to thank Dr. Rice for providing inspiration and insight throughout this project and the rest of the Rice research group for their support. I would also like to thank the collaborating engineering groups under the direction of Dr. Masoud Agah at Virginia Tech without whom this project would not be possible. These groups designed and fabricated the MEMS preconcentrators and the SPME fibers used in this project, and Dr. Agah provided advice for methods of evaluation. This work was supported in part through a grant from the National Science Foundation (GOALI Grant #0854242) and also through a summer fellowship at the College of William and Mary funded by the Howard Hughes Medical Institute.

List of Figures

Figure 1.1: MEMS Micropreconcentrator Chip Design.....	16
Figure 1.2: Preconcentrator Schematic.....	16
Figure 2: Examples of Micro-post Geometry and Orientation.....	19
Figure 3.1: Parabolic Reflector Design.....	20
Figure 3.2: Optical Image of a Preconcentrator with Webbed-Style Tenax Coating.....	20
Figure 3.3: SEM Image of a Preconcentrator with Webbed-Style Tenax Coating.....	20
Figure 3.4: Schematic of Parabolic Reflectors to Show Spacing Measurements.....	20
Figure 4: VOC Vented Vapor Setup.....	24
Figure 5: Valve Schematic for Adsorption and Desorption Modes.....	28
Figure 6: Schematic of SPME Fiber Holder for Headspace Analysis.....	31
Figure 7: Hexane adsorption/desorption chromatogram, duplicate 10:1 split runs for Precon #2.....	37
Figure 8: 1,1,2,2-tetrachloroethane adsorption/desorption chromatogram, duplicate 10:1 split runs for Precon #2.....	37
Figure 9: Chlorobenzene adsorption/desorption chromatogram, duplicate 10:1 split runs for Precon #5.....	44
Figure 10: Chlorobenzene adsorption/desorption chromatogram, duplicate 10:1 split runs for Precon #5.....	44
Figure 11: Chromatogram from chlorbenzene and 1,1,2,2-tetrachloroethane mix, 10:1 split for Precon #5.....	45
Figure 12: Chromatogram from 10-component VOC mix, 10:1 split for Precon #5.....	45
Figure 13: Hexane Adsorption/Desorption Profile, 10:1 split runs for Precon #6.....	48
Figure 14: Hexane Adsorption/Desorption Profile, 100:1 split runs for Precon #6.....	48
Figure 15: Chlorobenzene Adsorption/Desorption Profile, 100:1 split runs for Precon #6.....	48
Figure 16: 1,1,2,2-Tetrachloroethane Adsorption/Desorption Profile, 10:1 split runs for Precon #6.....	49
Figure 17: Chlorobenzene adsorption/desorption chromatogram, triplicate 10:1 split runs for Precon #8.....	52

Figure 18: 1,1,2,2-Tetrachloroethane adsorption/desorption chromatogram, triplicate 10:1 split runs for Precon #8.....	52
Figure 19: Chlorobenzene adsorption/desorption chromatogram, triplicate 10:1 split runs for Precon #9.....	55
Figure 20: Chlorobenzene adsorption/desorption chromatogram, triplicate 100:1 split runs for Precon #9.....	56
Figure 21: 1,1,2,2-Tetrachloroethane adsorption/desorption chromatogram, duplicate 10:1 split runs for Precon #9.....	56
Figure 22: 1,1,2,2-Tetrachloroethane adsorption/desorption chromatogram, duplicate 100:1 split runs for Precon #9.....	56
Figure 23: Hexane Adsorption/Desorption Profile, 10:1 split runs for Precon #11	59
Figure 24: Chlorobenzene adsorption/desorption chromatogram, 10:1 split runs for Precon #11	60
Figure 25: Chlorobenzene adsorption/desorption chromatogram, 100:1 split runs for Precon #11	60
Figure 26: 1,1,2,2-Tetrachloroethane adsorption/desorption chromatogram, 10:1 split runs for Precon #11	61
Figure 27: Pressure variation experiment, hexane 10:1 splits for Precon #11	63
Figure 28: Desorption Peak Area of Hexane as a Function of Time between Injection and Desorption for Precon #11	63
Figure 29: Chlorobenzene Adsorption/Desorption Runs, 10:1 Split for Precon #R100	65
Figure 30: Chlorobenzene Adsorption/Desorption Runs, 10:1 split for Precon #R200	67
Figure 31: Average masses of analytes retained by preconcentrators for adsorption/thermal desorption runs of 2.0 μ L injections at a 10:1 split flow	68
Figure 32: Average masses of analytes retained by preconcentrators for adsorption/thermal desorption runs of 2.0 μ L injections at a 100:1 split flow	69
Figure 33: Preconcentrator-to-Column Chromatograms using Precon #R200	70
Figure 34: Ten Component Mix Standard Calibration	72
Figure 35: Preliminary SPME chromatograms	72

List of tables

Table 1: Preconcentrator Labels and Specifications.....	19
Table 2.1: VOC Data	27
Table 2.2: VOC Volumes for Ten-Compound Vapor Mix	28
Table 2.3: VOC Densities and Volumes Used for 10.0 mL Standard Stock Preparation.	32
Table 3: Hexane Adsorption/Desorption Results for Precon #2	40
Table 4: Chlorobenzene Adsorption/Desorption Results for Precon #2	40
Table 5: 1,1,2,2-Tetrachloroethane Adsorption/Desorption Results for Precon #2	40
Table 6: Chlorobenzene Adsorption/Desorption Results for Precon #5	44
Table 7: 1,1,2,2-Tetrachloroethane Adsorption/Desorption Results for Precon #5.....	44
Table 8: Hexane Adsorption/Desorption Results for Precon #6	49
Table 9: 1,1,2,2-Tetrachloroethane Adsorption/Desorption Results for Precon #6	49
Table 10: Chlorobenzene Adsorption/Desorption Results for Precon #6	49
Table 11: Chlorobenzene Adsorption/Desorption Results for Precon #8	53
Table 12: 1,1,2,2-Tetrachloroethane Adsorption/Desorption Results for Precon #8	53
Table 13: Hexane Adsorption/Desorption Results for Precon #9	57
Table 14: Chlorobenzene Adsorption/Desorption Results for Precon #9	57
Table 15: 1,1,2,2-Tetrachloroethane Adsorption/Desorption Results for Precon #9.....	57
Table 16: Hexane Adsorption/Desorption Results for Precon #11	61
Table 17: Chlorobenzene Adsorption/Desorption Results for Precon #11	62
Table 18: 1,1,2,2-Tetrachloroethane Adsorption/Desorption Results for Precon #11	62
Table 19: Hexane Adsorption/Desorption Results for Precon #R100	65
Table 20: Chlorobenzene Adsorption/Desorption Results for Precon #R100	65
Table 21: 1,1,2,2-Tetrachloroethane Adsorption/Desorption Results for Precon #R100.	65
Table 22: Chlorobenzene Adsorption/Desorption Results for Precon #R200	66
Table 23: 1,1,2,2-Tetrachloroethane Adsorption/Desorption Results for Precon #R200.	66

Abstract

The goal of this project was to develop and carry out methods for evaluating a variety of Tenax-coated micro-preconcentrators and fused-silica solid phase micro-extraction (SPME) fibers for applications in micro-electro mechanical systems based gas chromatography. In the past, micro-preconcentration devices and SPME fibers have been fabricated and applied to gas chromatography (GC) systems. However, most of the preconcentration devices that utilized Tenax involved a packed form of the adsorbent polymer instead of the thin film surface coating and newly developed cobweb styles used in this project. Additionally, SPME fibers with Tenax as a sorbent were also of a new design and had not been extensively evaluated. Although time limitations prevented the extensive study of preconcentrators and SPME fibers, this project did suggest that the Tenax-based devices could feasibly be applied to micro-GC systems. Moreover, the methods developed in this project could be used for more extensive systematic evaluation in the future.

I. Introduction and Background

Gas Chromatography as an Analytical Tool: Gas chromatography (GC) is an analytical technique for the separation and determination of compounds with sufficient vapor pressure to exist in the gas phase at elevated temperatures [1]. This technique involves a gaseous mobile phase flowing in continuous contact with a liquid or solid stationary phase. Partitioning of a mixture of analytes between the two phases for compound-specific relative amounts of time drives the separation of analytes [2]. Gas chromatography can be utilized for isolation and identification of compounds as well as for preparative sample purification. Additionally, GC analysis can provide physicochemical constants such as entropy, enthalpy, free energy, and binding constants [2]. As a result of this versatile spread of both qualitative and quantitative analytical uses, GC applications span a wide range of fields including environmental studies, biochemical monitoring, hazardous material detection, forensic investigation, medical testing, pharmaceutical analysis, air quality monitoring, polymer characterization, petroleum research, pesticide residue determination, food chemistry, and toxicological studies [2-6].

Some of the benefits of GC analysis are the capability of achieving resolved separation of physically similar compounds, azeotropic mixtures, and structurally or chemically similar molecules [2]. The resolution can be optimized with appropriate stationary phase adsorbents for the separation of interest, and high separating power can be achieved because the low viscosity of the mobile phase enables the use of long separation columns [2,4]. Depending on the detector used, GC sensitivity can have limits of detection down to the parts-per-million or to sub-parts-per-billion ranges [2,3]. This

level of sensitivity is achieved with liquid sample volumes that are typically on the order of 1 μ L or less [2]. A variety of available detectors of GC instruments facilitates specialized, sensitive analysis [2-4]. Another advantage of GC is that the typical analysis time ranges from under 1 minute to over an hour depending on the application. Moreover, the convenience of system automation, the commercial availability, the market-competitive prices for instrumentation, and the ease of operation of GC systems enable practical and routine employment with potential for specialized applications [2].

Nevertheless, there are some limitations and disadvantages to standard GC techniques. With regards to instrumentation, conventional bench-top laboratory GC systems typically involve large components such as an oven, high pressure gas tanks, injection and detection hardware, and a standard computer or signal processor [1,4]. The size of these components and the high power requirements of GC systems render such instrumentation immobile [1]. The feasibility of field testing is thus limited by the requirement of reliable sample collection and transportation. Moreover, sample collection can often be time-consuming, unreliable, or expensive [4-6].

Innovations in GC systems have enabled the fabrication of portable gas chromatograph designs, which give rise to decreased analysis times as well as improved limits of detection [1,3]. The development of miniature or micro-GC instrumentation has generated progressively to more transportable systems [1,4,6]. Additionally, alternative ways of extracting and collecting samples have enabled more effective testing with both conventional and newly-innovated micro-GC systems [5-8].

Analysis of Volatile Organic Compounds: Volatile organic compounds (VOCs) are of interest in several analytical spheres, including food and fragrance chemistry, medicine, industrial hygiene, forensics, and environmental studies [2, 9]. A number of VOCs are present on the U.S. EPA priority pollutant list due to known toxicity and/or mutagenic and carcinogenic properties, so human health concerns are among the driving factors in the development of rapid analytical techniques for detecting and monitoring VOCs [9]. VOCs are also pertinent in atmospheric chemistry because they can deplete stratospheric ozone and form tropospheric ozone [11]. Repercussive effects of the influence pollutants such as VOCs on atmospheric composition are of rising concern in environmental and climate studies [12].

As a class of compounds, the VOCs incorporate a wide range of organic solvents and pollutants, all of which are either gaseous or easily volatilized under atmospheric conditions [11]. In comparison with other gas-phase analytical techniques such as differential optical absorption spectroscopy and membrane introduction mass spectrometry, GC is a more effective technique because of its versatility and capacity for analysis of complex mixtures of compounds [11]. Air sampling for GC analysis has been carried out with collection bags or canisters and more recently with sorbent extraction techniques [9,11]. In the case of the air bags or canisters, large volumes of air are required to detect low-level concentrations of analytes. Furthermore, this collection method is not reliable for all analytes as some compounds adsorb onto the inner walls of the container causing detected concentrations to be inaccurate, appearing lower than actual air concentrations at the time of sample collection. In the method of collection by analyte extraction from air via a sorbent phase, adequate equilibration time can be

lengthy. Additionally, compounds of similar polarity to the sorbent may interfere with the adsorption of the analytes of interest. For example, hydrophilic sorbent phases tend to collect water, which can hinder the reliability of analyte collection as well as the accuracy of the analysis [11].

Microelectromechanical Systems Based Micro-GCs: Micro-GC systems and improved analyte extraction/trapping techniques could both offer a means of improving the determination of VOCs in air [5-8,10]. Even the most recent functional micro-GC instruments, though portable, are still cumbersome for transportable on-site field work, and they are also still expensive to fabricate [13]. Commercially available micro-GC systems still have high power requirements, use large sample volumes, are costly to operate, and require relatively lengthy analysis times [1].

One area of recent research and development in micro-GC instrumentation involves innovations using microelectromechanical systems (MEMS) technology. Fabrication of micro-GC components via MEMS has the potential to offer considerable improvements in the development of efficient micro-GC systems. Specifically, some of the aims of applying MEMS technology to the fabrication of micro-GC instruments include increased system sensitivity, improved power efficiency, more ease of portability, and advancement toward multi-vapor *in situ* analysis [1, 4]. Recent work on the application of MEMS technology to micro-GC systems has been directed toward the development MEMS micropreconcentrator/focusers and MEMS micro-sized columns etched in serpentine patterns on silicon chips the size and thickness of a quarter. In conjunction, MEMS micro-analyzers/sensors for detecting gaseous compounds have been

recently fabricated as well, with one of the underlying objectives being to integrate all of the MEMS components into a complete, hand-held micro-GC system. Such fully integrated MEMS-based micro-instruments could replace conventional GC systems for analytical separations in field applications [4].

One noteworthy obstacle in micro-GC systems that could be resolved with MEMS innovation is the necessity of an analyte preconcentration step in order to detect lower concentrations of VOCs in air. Additionally, this innovation could allow for decreased power consumption and enhanced portability due to the small size of the components. Given that medical and environmental monitoring often require detection of compounds in the range of low parts-per-billion concentrations, the improvements that MEMS technology could offer in micro-GC systems could enable on-site analysis for applications in biomedicine, environmental monitoring, industrial assessment, and forensics/security due to improved limits of detection, [3-6].

Preconcentration: A preconcentration step is required in the analysis of VOCs in air via micro-GC systems to enable detection of trace concentrations of VOCs down to the part-per-billion range [4,8]. Concentrations this low might not otherwise be detectable just by passing an air sample through a micro-column. Furthermore, preconcentration can improve the quality of separations by focusing analytes to a small bandwidth before injection into a micro-column. The focusing effect of preconcentration gives rise to sharper, narrower peaks with better signal-to-noise ratios [6].

Preconcentration involves a collection phase in which either a static gas mixture or an air sample of interest comes into contact with an exposed adsorbent-coated fiber or a

known volume of gaseous sample is passed through an adsorbent-coated preconcentrator or an adsorbent-packed trap. In VOC analyses, analytes are usually trapped at or near ambient temperature. Following analyte collection onto a sorbent-coated surface, a rapid desorption phase releases the trapped compounds directly onto a GC column for separation. The subsequent release of accumulated analytes is usually achieved through thermal desorption where the preconcentrator, trap, or sorbent-coated fiber is rapidly heated to release the analytes [7,8]. Since this method of adsorption/thermal-desorption preconcentration gives a pulsed injection onto a GC column, improvement in peak resolution is usually obtained.

Essential to preconcentration is the adsorption of analytes, which is dependent on molecular interactions with surfaces. The adsorption process can be physical or chemical in nature. Physisorption involves intermolecular interactions such as Van der Waals, dipole, or hydrogen bonding whereas chemisorption entails stronger bonding interactions [10,11, 14]. Although both types of adsorption are affected by temperature, the conditions under which chemisorption occurs are more specific with respect to temperature and often limited to temperature ranges above the critical temperature of a gaseous compound [11]. The molecular interactions associated with physisorption are weaker, more reversible, and less specific than the interactions involved in chemisorptions. Additionally, chemisorption can only collect a monolayer of molecules whereas physisorption can involve multiple layers, which gives physisorption the potential for a higher capacity to hold analytes. On a micro-GC scale, physisorption is the more suitable mode of adsorption for an adsorbent in a preconcentration step because it allows for

collection of a range of analytes at ambient temperatures as well as rapid thermal desorption to then release analytes [11,14].

The properties of sorbents that can be used to select for specific analytes with regards to chemical properties include polarity, hydrophobic/hydrophilic character, and acidity/basicity [15]. Furthermore, for adsorbents with complex porous structures, the pore size of the material can also be important in selection for particular analytes [11,15]. However, due to the wide range of molecules with which many adsorbents can interact via physisorption, it is possible for adsorption sites to be occupied with molecules other than those of interest [6,11]. Since adsorption of non-target molecules can cause a decrease in the capacity of a preconcentrating surface for analytes of interest, specific adsorbent characteristics must be carefully considered [6].

MEMS-Fabricated Micropreconcentrators: MEMS preconcentrators for micro-GC systems are designed with internal adsorption sites that trap analyte compounds as ambient air is passed through. Subsequent rapid thermal desorption of the trapped compounds allows for a quick, pulsed introduction onto a separation column. Passing a known volume of sample gas through the adsorbent-packed or coated micropreconcentrator can allow for quantitative determination of analytes with respect to the original sample gas mixture.

Micropreconcentrators are geometrically constructed to be packed or coated with an adsorbent material for collecting analytes. Adsorbents can vary in chemical and physical properties and are selected depending on the desired types of analytes to be trapped for subsequent analysis. Carbon-based adsorbents of various surface areas and

pore morphologies such as the commercial absorbents CarbopackB, CarbopackX, and Carboxen 1000 from Supelco (Bellefonte, PA) as well as polymeric adsorbents, such as Tenax and microporous polystyrenes, have been used as adsorbents in MEMS-fabricated micro-GC instrumental components to collect VOCs of various volatilities [1,4,10]. Adsorbent polymers Chromosorb and Amberlite are more commonly used than Tenax in processes involving solvent desorption because Tenax has a lower volatile compound capacity [10].

Existing micropreconcentrator designs include glass and stainless steel capillaries with packed adsorbent beds [6]. In packed preconcentrators, layering the packing with adsorbent-coated beads from high surface area sites to low surface area sites enables the preconcentrator to progressively capture smaller molecules as gas flows through the adsorbent, which in turn increases efficiency of desorption and injection because smaller molecules that tend to be more volatile are trapped nearer to the column entrance than larger molecules [6]. Another design involves parallel slats of deep-reactive-ion-etched silicon arranged on a silicon-doped membrane and packed with adsorbent [4]. For the purposes of analyzing complex mixtures of gases, multiple adsorbents can be applied to a single preconcentrator [4, 6].

Quantitative preconcentration can either be based on adsorbent-analyte equilibrium or on maximum adsorbent capacity. An isothermal curve relating the quantity of adsorbed analyte to either the pressure or the concentration of the analyte in the mobile gas phase at constant temperature represents a characteristic descriptor of an adsorption system [11]. If an analyte is in equilibrium with the sorbent, then the amount of trapped analyte can be determined from sorbent volume, and analyte concentration in the sorbent

phase. Analyte equilibrium with a stationary phase can describe analyte interaction with a sorbent phase at low concentrations when there is a linear sorption isotherm [16].

Preconcentration based on this principle would have to involve concentrations of analyte that were below the sorption capacity for the given adsorbents. The practical advantage of equilibrium preconcentration as opposed to exhaustive preconcentration is that the volume of sample does not need to be specified in order to determine the amount of analyte in the preconcentrator. However, isothermal adsorption curves are not always linear, and more complicated equations and models for quantitative analysis can be used to describe multilayer sorption and sorbent-systems with multiple pore sizes or surface areas [11, 16].

Complete or exhaustive adsorption, as opposed to equilibrium adsorption, involves using an adsorbent with a large enough partition coefficient and capacity to trap all of the analyte of interest that passes through the preconcentrator. Accordingly, the sample volume injected into the preconcentrator must be known in order to determine the concentration of analyte in the sample. This method of preconcentration is effective up until volumes at which the capacity of the adsorbent is reached and a portion of analyte is lost because it passes or breaks through the preconcentrator without being trapped. Due to stronger adsorption characteristics, these systems are capable of collecting more analyte than preconcentrators based on equilibrium adsorption, but the thermal desorption phase for these exhaustive preconcentrators requires a larger increase in temperature to overcome the sorption interactions and release the collected analytes [1, 11, 16,17].

In terms of assessment, preconcentrators can be evaluated with regards to the capacity of adsorbent to trap analyte and the efficiency of the desorption phase [6]. The

breakthrough volume of an adsorbent coating is the maximum volume of sample that can be passed over the adsorbent with complete retention of all analyte, or the point past which analyte would begin to be eluted instead of adsorbed [15]. The capacity of an adsorbent-coated preconcentrator to trap analytes is thus directly related to the breakthrough capacity. The breakthrough capacity depends on the flow rate of mobile samples as well as on the adsorbents and analyte concentrations used [11,17].

In addition to evaluating attributes of specific adsorbents used in preconcentrators, the effectiveness of a preconcentrator can be evaluated with respect to the microGC system as a whole. The rate of thermal desorption from the preconcentrator directly influences the injection bandwidth, which in turn affects the number of theoretical plates for separation within the microcolumn. A rapid change in temperature brought forth by innovative micro-heaters built into preconcentrator structures encourages fast desorption which gives rise to a narrower injection band and allows for a greater number of theoretical plates [7, 8, 15]. Additionally, flow rates, injection volumes, and temperature programming can be adjusted for study of preconcentrators integrated into microGC systems. The resulting peak heights, peak-widths at half height, and peak resolution can be used to characterize the effects of the increased pulse concentration of analyte released from the preconcentrator [8].

Problems encountered with preconcentrators can arise from both design and application. Peak tailing has been encountered, possibly due to desorption properties of the adsorbents used and the analytes under examination [17]. This problem can be resolved by increasing the temperature of desorption to ensure that all analyte is released from the preconcentrator at approximately the same time. The risk of operating

preconcentrators at higher temperatures is that degradation of adsorbent or sample may occur to some extent. [16]

Another problem is exceeding the breakthrough capacity, which means that all adsorption sites in the preconcentrator become occupied and subsequent analyte passes through instead of being collected on the preconcentrator. Intensive studies of breakthrough points for various adsorbent materials have been in the design of micro-preconcentrators fabricated to test solutions of concentrations below the limits of the maximum capacity of the internal adsorbent [17].

In engineering and design, the connection of the preconcentrator to the systematic micro-GC flow must be leak-proof without causing excessive backflow, which has been accomplished with the application of fused silica capillaries and polyimide sealant [2].

One branch of research aimed at improving preconcentrator efficiency is the novel incorporation of nano-structured adsorbents into a MEMS-fabricated preconcentrator. It has been suggested that control of thermal desorption could be improved using such adsorbents, which would increase preconcentrator effectiveness and overall system power efficiency [14]. Future studies may explore chemical properties of nano-adsorbents in microGC preconcentrators, selectivity for analytes of interest, and optimization of preconcentrator capacity.

Solid-Phase Microextraction: Solid-phase microextraction (SPME) is a sorbent-based technique used for sample collection. As opposed to whole-air sampling, which involves collecting air in a bag or canister, SPME traps only analytes and thus serves as a simultaneous sample collection and preconcentration method [9]. The technique involves

a polymeric sorbent-coated silica piece of fused silica fiber [19]. A syringe-like holder can be used to sheath a coated fiber inside of a hollow needle. The holder has a spring-loaded plunger to control whether the fiber is contained within the holder needle or protruding out of the needle tip and thus exposed. To collect and preconcentrate analytes, the coated fiber is exposed to a gaseous or liquid sample long enough for adsorption equilibration. After analytes adsorb to the surface of the polymeric coating during this collection step, the fiber is then pulled back into the needle. The syringe-like holder is then used to inject the preconcentrated sample into a GC by piercing the septum of the injection port with the holder needle and then immediately exposing the fiber inside. The heat of the injection port thermally desorbs the analytes, which are then directed through the GC by a carrier gas flow [18]. Since the GC injection port is constantly heated to temperatures high enough to thermally desorb analytes from a polymeric sorbent surface, the insertion of the SPME fiber should give rise to a quick, pulsed release of analyte in a manner similar to that of preconcentrator desorption of analytes. After analysis the coated fiber can then be reused, making the technique cost-efficient [18].

Serving as a preconcentration technique, SPME is used in combination with GC analysis similarly to micropreconcentrators. However, the SPME syringe is more easily transportable and less expensive to fabricate than a micro-GC system with an integrated micropreconcentrator. The SPME technique could thus be used either with either conventional or micro-GC systems. Applications of SPME are comparable to those of micropreconcentrators and include analysis of human breath for medically relevant volatile compounds, industrial hygiene, and environmental air sampling [9, 18].

Commonly used polymer coatings for SPME fibers include polydimethylsiloxane (PDMS), Carbowax-divinylbenzyl, and PDMS-divinylbenzyl, all of which are useful in adsorption-based applications [19]. Additionally, active carbon-based coatings that have also been used in SPME for air analysis include Carboxen and Carbopack B (Supelco) [9]. PDMS-coated SPME fibers have the advantages of an extended linear dependence range between the amount of analyte retained on the fiber and the sample concentration and low rates of degradation of unstable analytes [19]. Moreover, PDMS has independent retaining capacities for analytes, so individual analytes have their own partition coefficients with PDMS which are not influenced by the presence of other analytes [19].

Tenax: Tenax is a commercially-available linear polymer that has been used in gas chromatography as a stationary phase and in air analysis as an adsorbent material [20]. The polymer has a relatively high thermal stability up to 350°C and a low adsorption affinity for water [20]. The overall low adsorption capacity of Tenax compared to other polymeric sorbents restricts its application in high-concentration environments, but it can often be more useful in low-concentration environments [10]. For this reason, it might be a useful sorbent in preconcentration and SPME applications in micro-GC applications. It has been reported that Tenax TA used for purge and trap adsorption with thermal desorption has breakthroughs volumes of hexane, chlorobenzene, and 1,1,2,2-tetrachloroethane in increasing order [21]. Although Tenax has been used in packed sorbent traps and air tubes, no systematic evaluations of Tenax thin films applied as adsorbents have been conducted, and little quantitative information has been published on the physical properties and VOC adsorption mechanisms of Tenax [2, 20].

Purpose: The intent of this study was to develop methods to evaluate thin film and webbed-style Tenax-coated micropreconcentrators as well as thin film Tenax-coated SPME fibers for applications in MEMS-based gas chromatography systems. This project was a part of a collaborative research effort with the research group of Professor Masoud Agah from the Department of Electrical and computer Engineering at Virginia Tech where the Tenax coated preconcentrators and SPME fibers were produced. Specifically, this project had an experimental focus on the ability of preconcentrators and fibers to collect and thermally release volatile organic compounds in the vapor phase. The work on preconcentrators is intended to be a preliminary evaluation of function and design, which will serve to direct the engineering of new designs and sorbent coatings. The aim of the fiber investigation is to evaluate the performance of Tenax in SPME applications.

II. Experimental Parameters and Procedures:

MEMS-based Micro-Preconcentrator Design and Fabrication: MEMS-based micro-

preconcentrators were produced from silicon wafers via highly elaborate plasma etching techniques at the Virginia Tech MEMS facility. Each of the preconcentrator chips examined in this study was fabricated in a roughly square shape with edges of approximately 1.0cm in length. A depression into the majority of the interior area of the chip created a rectangular cavity surrounded by the remaining edge around the perimeter of the chip. Two fluidic ports on opposite edges of the preconcentrator were etched through points of the cavity wall to enable gaseous flow via capillary connections.

The preconcentrator cavity was etched in such a way that 20 μ m-wide silicon micro-posts remained within the cavity, an innovation with the purpose of increasing total surface area inside the preconcentrator. The posts stretched the entire height of the internal cavity. The preconcentrator design was such that gas would flow into one fluidic port, through and around the microposts, and out the other fluidic port on the opposite side of the internal cavity. The preconcentrators were symmetrical, so the direction of flow was arbitrary and reversible. Figure 1.1 consists of mockup images that show three close-up views of an artist's rendition of an etched preconcentrator chip with fluidic ports and embedded micro-pillars.

Following the cavity etching and micro-post formation, a Pyrex wafer was anodically fused to the top cross-section of the etched chip to seal off the preconcentrator, and thus rendering the sample entrance and exit ports on the sides as the only openings to the micropreconcentrator. Figure 1.2 is a schematic that shows the placement of cut and fitted Pyrex onto the chip. The pyrex-sealed preconcentrators were rectangular prism-shaped and had approximate internal dimensions of 1.0cm x 1.0cm x 250 μ m.

Figure 1.1: MEMS Micropreconcentrator Chip Design

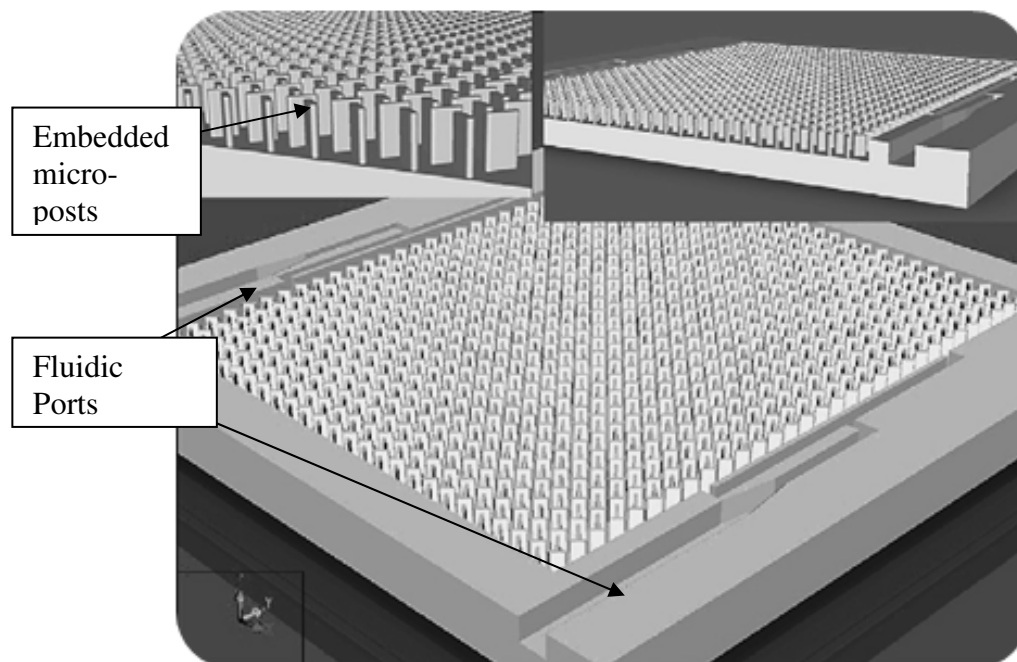
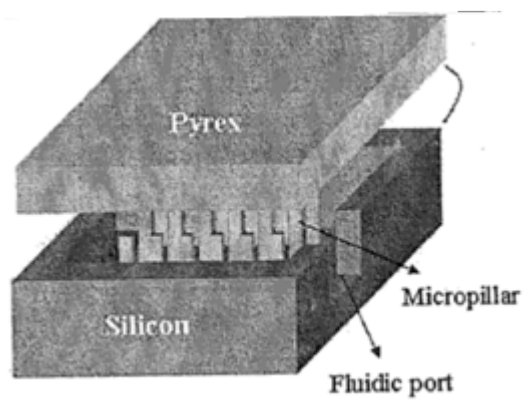


Figure 1.2: Preconcentrator Schematic



After the Pyrex seal was mounted, the preconcentrators were either left uncoated or were coated with the Tenax adsorbent. The Tenax coating for the preconcentrators was applied in either a surface-precipitation style or a webbed style. In the surface coated preconcentrators, the Tenax adhered in a layer on the internal surface area to cover all inside faces of the Pyrex-sealed chip as well as the surfaces of any added geometrical features such as the microposts or split fluidic ports. In the web-coated preconcentrators, parabolic reflectors were embedded instead of micro-pillars, and the Tenax was spindled into a three dimensionally webbed network affixed to internal faces. The meshed polymer in the latter style of polymeric coating resembled an intricate cobweb.

The micro-pillars embedded in the preconcentrators were designed with variable geometries and orientations. The posts could be square, circular, or oblong. The rows of square or circular posts were labeled as “ordered” when the posts from row to row were all aligned, and the rows were considered “staggered” if alternating rows were offset such that the posts were not aligned from row to row. The oblong posts were oriented in a criss-cross orientation. Figure 2 is a diagram that shows an above-chip view of some of the possible combinations of post geometry and post orientation. Other possible combinations of post geometry and orientation that were tested but not shown in Figure 2 include square staggered or circle ordered designs. Table 1 summarizes the specifications of the preconcentrators that were fabricated for evaluation in the scope of this project. Each preconcentrator had a numeric label for identification purposes. The webbed preconcentrators did not have “post-spacing” values because of their unique parabolic etched design shown in Figure 3.1. Figures 3.2 and 3.3 show images of the webbed-style Tenax attached to parabolic reflectors, and Figure 3.4 is a diagram that

demonstrates the “side” and “middle” spacing measurements listed for the webbed preconcentrators in Table 1.

Figure 2: Examples of Micro-post Geometry and Orientation

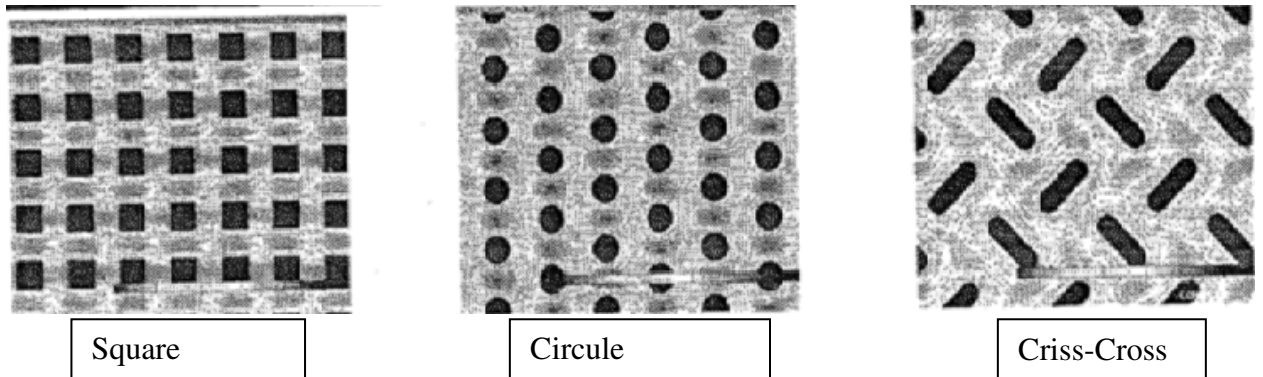


Table 1: Preconcentrator Labels and Specifications

<u>Preconcentrator Label</u>	<u>Post Geometry</u>	<u>Post Spacing (μm)</u>	<u>Coating Method</u>
1	Criss-Cross	100	25 mg/mL Tenax precipitation
2	Criss-Cross	10	uncoated
3	Square Staggered	10	uncoated
5	Circule Staggered	50	25 mg/mL Tenax precipitation
6	Circule Ordered	50	25 mg/mL Tenax precipitation
7	Criss-Cross	10	uncoated
8	Square Ordered	50	25 mg/mL Tenax precipitation
9	Circule Staggered	100	25 mg/mL Tenax precipitation
10	Square Staggered	10	uncoated
11	Criss-Cross	50	25 mg/mL Tenax precipitation
R100	Parabolic	Middle: 100 Side: 250	Tenax webbing
R200	Parabolic	Middle: 200 Side: 200	Tenax webbing

**Designs in bold were evaluated in this study

Figure 3.1: Parabolic Reflector Design

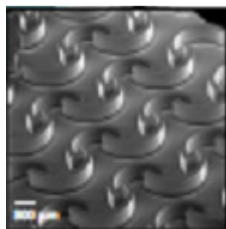


Figure 3.2: Optical Image of a Preconcentrator with Webbed-Style Tenax Coating

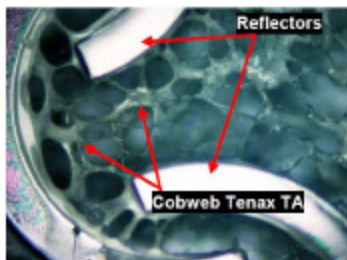


Figure 3.3: SEM Image of a Preconcentrator with Webbed-Style Tenax Coating

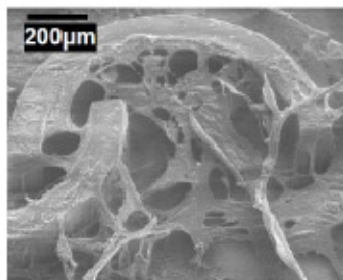


Figure 3.4: Schematic of Parabolic Reflectors to Show Spacing Measurements



All of the MEMS-based micropreconcentrators evaluated in this project were designed, fabricated, coated with polymeric adsorbent, and attached with polyimide sealant to capillary connection pieces by the collaborating groups under the direction of Dr. Masoud Agah at the Virginia Polytechnic Institute and State University. The loose ends of the capillary column were septum-sealed for preconcentrator shipping and storage.

Experimental Instrumentation for MEMS Preconcentrator Tests: A conventional benchtop Agilent 6980 gas chromatograph was used for preconcentrator evaluation. The injection port was heated to 250°C and held at constant temperature throughout experimentation. The GC had a split/splitless inlet, and both of these flow modes were utilized. Helium was used as the carrier gas. For the detection of analytes, a flame ionization detector was used at a temperature of 250°C.

Adsorption/Desorption Testing Setup: Preconcentrators had two pieces of standard 0.25 mm diameter deactivated fused silica capillary column connected to the fluidic ports to enable attachment to a conventional gas chromatograph. The total length of the two connection pieces plus the length of the preconcentrator chip together was standardized to approximately 1.0 m for all preconcentrator chips. One piece of the capillary connector was attached to the GC inlet and to one fluidic port of the preconcentrator chip, and the other connection piece was attached to the opposite fluidic port of the preconcentrator chip and to the flame ionization detector (FID). The connections to the GC inlet and FID were made using graphite sealed ferrules and standard GC nuts.

The preconcentrator chip was fastened flat against a small resistively heated panel using a paper clip. The resistive heating panel was connected on a circuit to a multi-meter and an on/off switch. The temperature of the chip was correlated to voltage generated from a thermoresistor such that 10.0 mV corresponded to the panel temperature reaching ~250°C. This setup allowed for rapid heating of the chips, which was intended to accommodate thermal desorption of analytes adsorbed to the preconcentrator coating. The heater circuit had to be shut off after the voltage reached 10.0 mV to avoid overheating and degradation of the capillary column seals. The panel did not stay at the elevated temperature once the circuit was shut off and instead cooled back to ambient temperature. Voltage readings were used to confirm the decrease in temperature and the return to a stable ambient temperature that followed the switching of the circuit from the on to off position.

GC Flow Calibration for Preconcentrator Testing Setup: A 10.0 mL bubble-meter was used to calibrate gas flow through the GC in the setup with the preconcentrator connected. A soap film bubble was prepared, and the time of travel for a given volume of 1.0 or 10.0 mL was taken with a stop-watch. The rate of bubble movement was translated into a flow-rate in milliliters per minute. The GC system pressure was adjusted to obtain a 1.0mL/min flow rate for all preconcentrator chips.

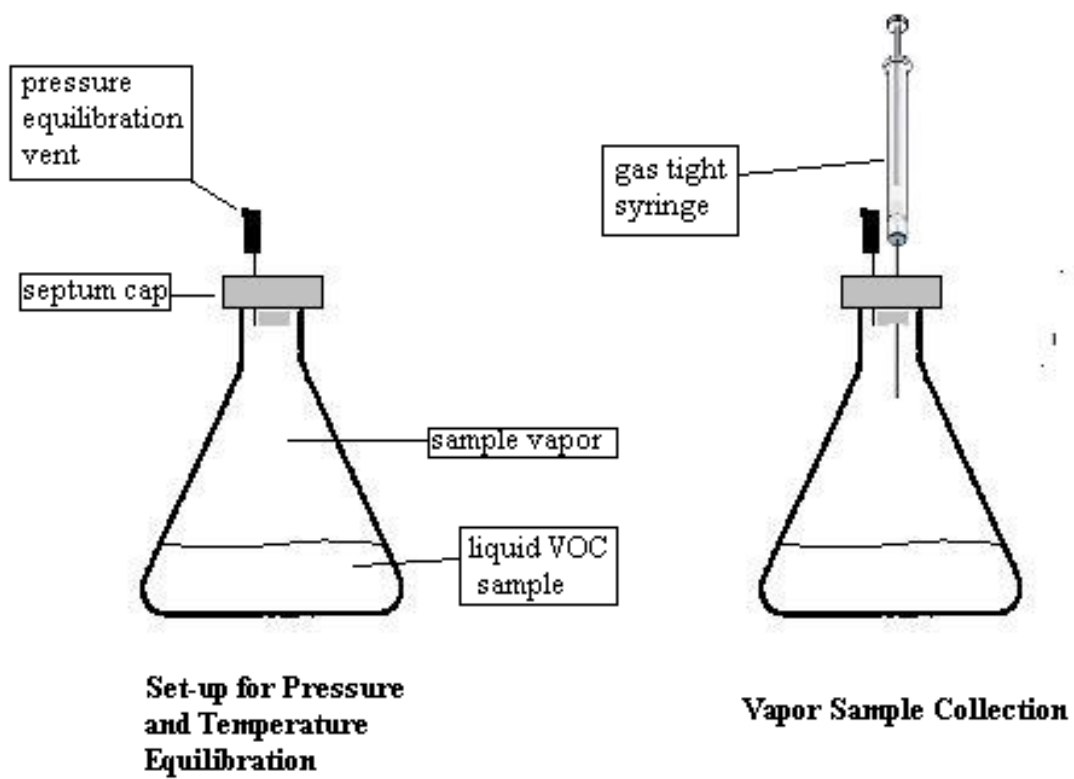
Blank Preconcentrator Heating: The MEMS preconcentrator chips that were directly connected to GC inlet and detector via capillary column attachment pieces were purged

with helium carrier gas until a stable background signal was observed from the FID. The chips were then rapidly heated to 250°C with the resistive heating system.

The blank heating runs were conducted primarily in order to clean the preconcentrators by thermally desorbing trapped volatile contaminants, but were also used as a background control for comparison.

Reagent Preparation for Preconcentrator Experiments: Vaporous samples of hexane, 1,1,2,2-tetrachlorethane, and chlorobenzene were prepared for preconcentrator testing. Sample preparation involved placing ~10 mL of each compound into separate 25 mL Erlenmeyer flasks, sealing the flask with a septum cap, and then inserting a hypodermic syringe needle through an edge of the cap to create a pressure equilibration vent when in use. Samples were left sitting on a bench for at least 30 minutes prior to their usage in order to allow for equilibration of the VOC vapor with atmospheric pressure and room temperature to ensure that the headspace was purged of air by the volatile compounds. A 10.0 µL gas tight syringe was then pierced through the center of the septum cap and used to collect vaporous samples in volumes between 1.0 and 5.0 µL. Figure 4 shows the vapor sample setup for equilibration and sample collection.

Figure 4: VOC Vented Vapor Setup



Preconcentration of VOCs (Adsorption/Thermal Desorption): MEMS preconcentrators were connected to the GC and attached to the resistive heating panel as previously described in the testing setup. Two blank heating runs were conducted prior to beginning breakthrough capacity runs to ensure a clean preconcentrator. After blank heating, a preconcentrator was considered ready for testing when the resistive heater had cooled to ambient temperature and a steady background FID signal was observed.

The two phases of preconcentration were collection and thermal desorption. The collection or adsorption phase involved the injection of vaporous compound samples into the GC injection port with a gas-tight syringe. Under the pressured flow of the helium carrier gas, samples traveled through the GC inlet and the first capillary connection to the Tenax-coated preconcentrator. Although the GC injection port was heated to 250°C, the MEMS preconcentrator was at a temperature of between 30°C and 40°C during this phase in the GC oven, and the resistive heating panel circuit was in the off position. As helium carrier gas flowed through the preconcentrator, VOC analytes were adsorbed onto the surface of the polymeric Tenax stationary phase. Any FID signal obtained that was above the baseline during the collection phase was considered breakthrough signal resulting from a portion of VOC analyte that passed through the preconcentrator instead of being trapped on the Tenax coating.

Following the analyte collection phase, the thermal desorption phase was conducted. If there was a breakthrough peak present in the FID signal during the collection phase, then the initiation of the desorption phase was delayed until a steady baseline signal was observed. The resistive heating circuit was then turned on using a switch located outside of the GC oven. The circuit was left on until the resistive heating

panel reached approximately 250°C. Heat was readily transferred from the heating panel to the silicon preconcentrator chip and rapidly released the VOCs that had been trapped during the collection phase. The VOC analytes were then carried through the second piece of capillary column connection directly to the flame ionization detector by the carrier gas flow. Chromatogram profiles of the entire process, adsorptive collection followed by thermal desorption, were obtained and saved. Peaks on the chromatograms were integrated to give signal areas. Peak-heights, peak-widths, and retention times were also collected and saved.

Timed Adsorption/Desorption with MEMS Preconcentrators: The time between breakthrough peak appearance and thermal desorption initiation was varied between 2.0 min and 12 min. Time was measured starting from the appearance of breakthrough maxima and stopping with the rapid thermal desorption by switching on the heating panel.

Preconcentrator-to-Column Coupling: Both capillary connection ends of a preconcentrator were connected to a 6-way fluidic valve. Also connected to the valve were both ends of a standard 15m x 0.25 mm i.d. capillary column with a 0.25 µm thick methyl silicone stationary phase coating (Restek), a capillary connection to the GC inlet, and a capillary connection to the FID. The entire valve set-up was contained in the GC oven, and the preconcentrator was fastened to the resistive heating panel. Figure 9 shows a schematic diagram of the valve, which could be switched between two different modes of operation. The adsorption mode involved flow from the inlet, through the preconcentrator, and then to the FID without passing through the column. The injection

port was held at constant temperature 250°C, and the oven temperature was set to 35°C. The system pressure was set to 1.2 psi during the adsorption phase.

A 10-component VOC vapor mixture containing dichloromethane, chloroform, carbon tetrachloride, dibromomethane, toluene, tetrachloroethylene, chlorobenzene, p-xylene, 1,1,2,2-tetrachloroethane, and bromobenzene was prepared prior to experimentation. The mixture was prepared in a 25.0mL Erlenmeyer flask. The analyte volumes required for each compound were determined from the respective vapor pressures of each compound at ambient temperature such that each was sufficiently volatilized and would produce chromatographic peaks at comparable levels. Table 2.1 shows molecular masses, boiling points, and densities of the VOCs, and Table 2.2 summarizes the volume requisites from vapor pressures.

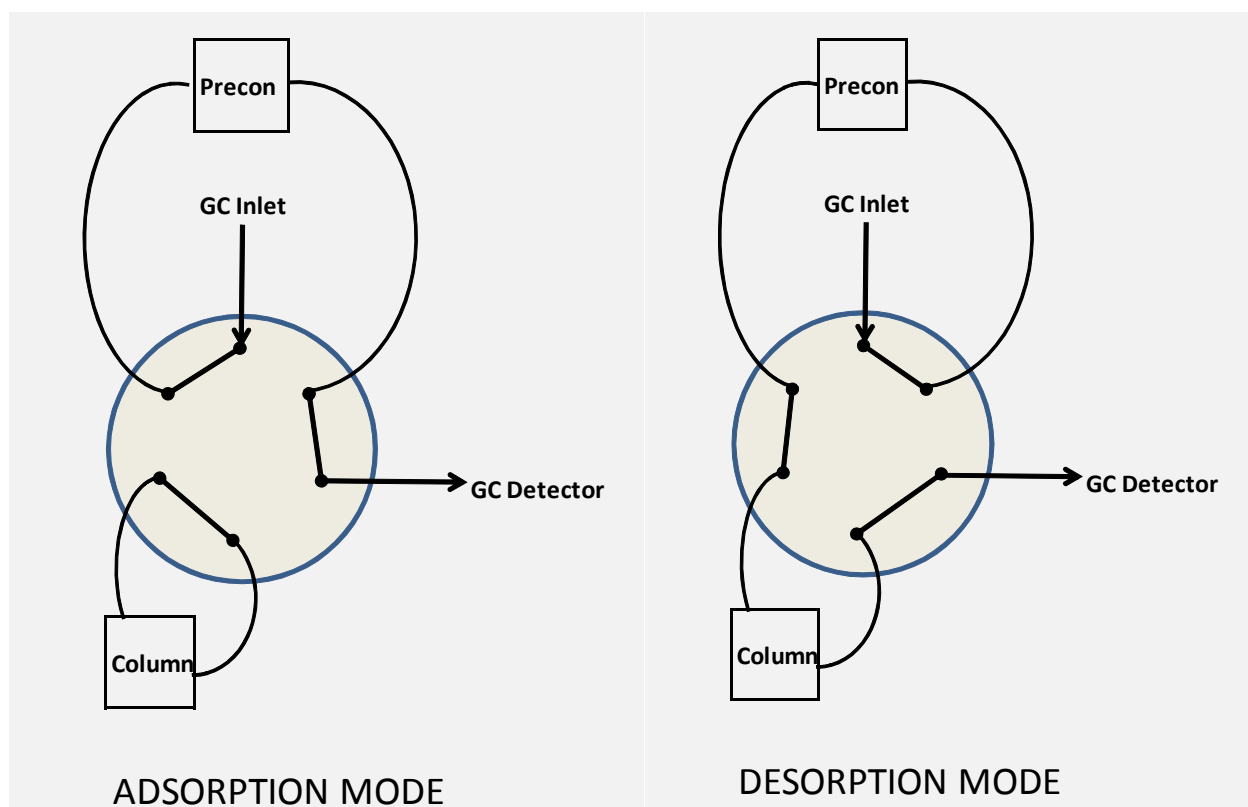
Table 2.1: VOC Data

Compound	Molar Mass (g/mol)	Boiling Point (°C)	Density (g/cm³) at 20°C
Methylene chloride	84.933	40.0	1.32662
Chloroform	119.378	61.17	1.483
Carbon tetrachloride	153.823	76.8	1.594
Dibromomethane	173.835	97	2.4969
Toluene	92.139	110.63	0.8669
Tetrachloroethylene	165.833	121.3	1.623
Chlorobenzene	112.557	131.72	1.1058
p-Xylene	106.165	138.23	0.8565
1,1,2,2-Tetrachloroethane	167.849	145.2	1.5953
Bromobenzene	157.008	156.06	1.495
1,2-Dichlorobenzene	147.002	180.0	1.3059

Table 2.2: VOC Volumes for Ten-Compound Vapor Mix

Compound	Vapor Pressure (kPa) at 20°C	Volume Used (mL)
Methylene chloride	47.4	0.1
Chloroform	21.2	0.1
Carbon tetrachloride	12.2	0.1
Dibromomethane	5.0	0.1
Toluene	3.8 (at 25°C)	0.5
Tetrachloroethylene	1.9	0.5
Chlorobenzene	1.17	1
p-Xylene	0.82	2
1,1,2,2-Tetrachloroethane	0.647	2
Bromobenzene	.55 (at 25°C)	2

Figure 5: Valve Schematic for Adsorption and Desorption Modes



The flask contained approximately 10 mL of VOC mixture and was capped with a rubber stopper. A hypodermic syringe needle was used to make a vent through the stopper, which allowed for atmospheric pressure equilibration. Equilibration with ambient temperature was achieved by leaving the vented flask sitting at room temperature for at least 30 minutes.

Varying volumes of the VOC mixture on the order of 1 to 10 μ L were withdrawn from the headspace of the flask and injected into the GC with the valve set to the adsorption mode. Following a breakthrough FID signal and a return to a steady baseline, the valve was switched to the desorption mode, to direct the flow through the inlet, preconcentrator, 15m capillary column, and then to the FID. When the valve was switched, the system pressure was increased to 15 psi, to give a flow of 2-3 mL/min in the column. After the system pressure increase, approximately 1 min was allowed for pressure equilibration prior to desorption. The resistive heater was then switched on, and the preconcentrator was heated to approximately 250°C. A chromatogram was obtained from the desorption and subsequent separation.

Solid Phase Micro-Extraction (SPME) Fiber Coating: The Agah group at Virginia Tech was responsible for coating fibers with Tenax for evaluation. Silica fibers of 1cm in length and 125 μ m in diameter were rinsed with acetone and then dipped into a solution of Tenax TA to coat the fibers. The coating solution was prepared by dissolving Tenax TA (Sigma-Aldrich Inc., St. Louis, MO) in dichloromethane up to concentration of 100mg/mL. After the fibers were dipped in the solution, they were slowly withdrawn

from the solution and then dried in ambient air. The thickness of the sorbent film coating ranged from 7 to 100 μm .

SPME Fiber Holder: A manual SPME fiber holder (Sigma-Aldrich Inc., St. Louis, MO) was used in the evaluation of the coated fibers. The syringe-like holder sheathed a fiber inside of a hollow needle that could be used to pierce septa. A spring-loaded plunger could be pushed down to force the fiber out of the tip of the needle for exposure to the air. A notch on the side of the holder allowed for the fiber to be locked in the exposed position. When unlocked, the spring pushed the fiber back into the needle, and the plunger could be manually pulled back fully to the top position in order to completely sheathe the fiber. The holder enabled adjustment of the length of fiber that protruded when locked in the exposed position. This length was adjusted such that all of the coated part of the fibers being tested would be exposed. Once adjusted, the length was not changed again. Figure 6 is a schematic diagram of the SPME fiber holder.

SPME Reagent Preparation: A ten-compound VOC mix containing dichloromethane, chloroform, carbon tetrachloride, dibromomethane, toluene, tetrachloroethylene, chlorobenzene, p-xylene, 1,1,2,2-tetrachloroethane, and bromobenzene were prepared in both pentane and in methanol. All components of the solutions were reagent grade (Sigma-Aldrich Inc., St. Louis, MO). To prepare the two stock solutions, 9 mL of solvent (either pentane or methanol) was poured into a 10.0 mL glass volumetric flask, and a volumetric syringe was used to spike the solvent with the appropriate volumes of VOCs. Each flask was then filled to the 10.0 mL mark with solvent, capped with a glass stopper,

then shaken and inverted to mix the solutions. The stock solution concentration was 10000 ppm (mass/volume), and volumes of solutes were determined from values for density near ambient temperature (20°C to 25°C). VOC densities and the calculated volumes required for spiking the stock standard are shown in Table 2.3.

Figure 6: Schematic of SPME Fiber Holder for Headspace Analysis

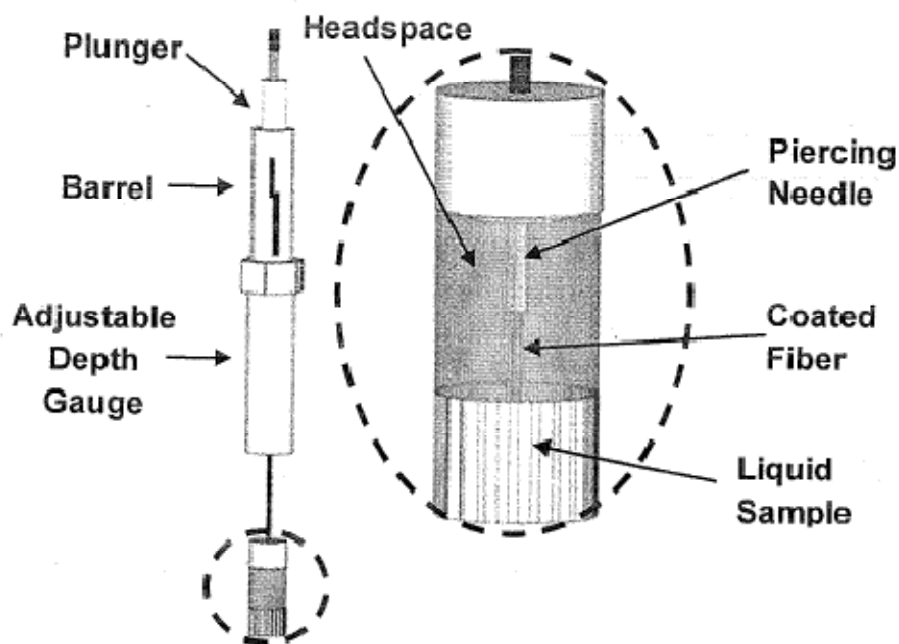


Table 2.3: VOC Densities and Volumes Used for 10.0 mL Standard Stock**Preparation**

Compound	Density (g/cm³) at 20°C	Volume (μL) equivalent to 100mg
Methylene chloride	1.32662	75.4
Chloroform	1.483	67.4
Carbon tetrachloride	1.594	62.7
Dibromomethane	2.4969	40.0
Toluene	0.8669	115.4
Tetrachloroethylene	1.623	61.6
Chlorobenzene	1.1058	90.4
p-Xylene	0.8565	116.8
1,1,2,2- Tetrachloroethane	1.5953	62.7
Bromobenzene	1.495	66.9
1,2-Dichlorobenzene	1.3059	76.6

Sequential one-to-ten dilutions by volume of the stock solution were used to make a series of solutions with concentrations of 1000ppm, 100ppm, 10ppm, 1ppm, 0.1ppm, and 0.01ppm. To make each dilution, 8mL of solvent was placed in a 10.0mL volumetric flask, a volumetric pipette was used to add 1.0mL of the solution with a concentration ten times greater than the desired concentration. The contents of the flask were then topped off with solvent to the 10.0mL mark. The flasks were capped with glass stoppers, and the solutions were mixed. One series of solutions was made in pentane, and another series was made in methanol. All standards were refrigerated when not in use to minimize evaporation.

Experimental Instrumentation for SPME Fiber Tests: SPME fiber evaluation was

conducted with a conventional benchtop Agilent 6980 gas chromatograph coupled to an

Agilent mass spectrometer (MS). The injection port was heated to 280°C and held at constant temperature throughout experimentation. The GC had a split/splitless inlet, but only the splitless mode was utilized. Helium was used as the carrier gas. A 30 m x 0.25 mm DB-1 coated capillary column (Agilent) was used for all SPME GC-MS tests.

Standard GC-MS Runs: A conventional 10.0µL liquid syringe was used to make 1.0 µL injections of the VOC standard solutions prepared in pentane. A chromatogram was obtained, and mass spectra were used to confirm the identity, elution order, and peak areas relative to concentration of the VOCs.

Thermal Fiber Cleansing: After installation of a Tenax-coated fiber into the SPME fiber holder, the fiber was placed in the sheathed position, and the holder needle was used to pierce the septum of a heated GC injection port. The holder plunger was then depressed, and the fiber was locked in the exposed position. The exposed fiber was left in the heated GC injection port for at least one hour before beginning experimentation to allow ample time for adsorbed contaminants to be thermally desorbed from the Tenax sorbent coating. The hour-long cleansing was only used at the very beginning of experimentation and subsequently when the fiber had been sitting out for more than a day, even if the fiber was sheathed in the holder. Otherwise, a thermal cleansing of at least ten minutes was conducted in between experimental trials. To avoid contamination from ambient air, the fiber was left exposed in the heated GC port until it was time to run an experiment, at which point the fiber was sheathed, and the holder was removed from the GC port.

Headspace Analysis: Sample preparation for SPME vapor trapping experiments involved filling a 60 mL test tube with 40.0mL of deionized H₂O. A PTFE double cross-head stir bar and 12.5g NaCl were placed in the test tube as well. The test tube was then capped with either a rubber stopper or a twist-on septum-holding cap with a Teflon septum inserted. With the sealed cap, there was an approximate headspace volume of 10.0 mL inside the test tube above the liquid. A 100 μ L syringe was used to spike the water with 40.0 μ L of a VOC solution prepared in methanol. The test tube was then clamped to a ring stand so that the liquid-containing portion of the tube was submerged in a beaker of room temperature water sitting on a multi-function hot plate and stirrer.

For headspace analysis, the SPME fiber holder with the fiber in the sheathed position was used to pierce the cap of the test tube. The holder was clamped above the test tube. The plunger was then pushed down, and the fiber was locked in the exposed position for 30 min. The solution was stirred during this time. Some trials were heated as well, but most were conducted at ambient temperature. After the 30 min collection period, the fiber was re-sheathed into the holder. The holder was immediately removed from the test tube cap and inserted into the heated injection port of the GC-MS, where the fiber was once again exposed to enable the thermal desorption, separation, and detection of analytes. A chromatogram was obtained from each run.

During the first few trials the clamp heights were carefully adjusted so that the fiber tip would extend down into the headspace close to the water but not in contact with the liquid at all. The clamp heights were marked and left unmoved for the remainder of experimentation.

III. Results and Discussion: MEMS Preconcentrator Evaluation

Of the twelve MEMS preconcentrators to be evaluated, the coated preconcentrators were prioritized for experimentation. One uncoated preconcentrator (#2) was evaluated for the purpose of comparison with the coated preconcentrators. However, due to time constraints, no other uncoated preconcentrators were evaluated in this study. Additionally, not all of the tested preconcentrators endured the full process of experimentation. Leaks in the sealed connection between the fluidic ports and the capillary column pieces or cracks in the Pyrex cover rendered some of the preconcentrators nonoperational. Also, given the setup in a conventional GC, breakage of the capillary connection pieces sometimes resulted in connection pieces that were too short to span the length from the GC inlet to the preconcentrator and then to the detector. In these cases, preconcentrators could no longer be installed into the GC. Enough testing for data collection was carried out on the preconcentrators listed in bold that were previously shown in Table 1.

Preconcentrator #2: With preconcentrator #2 setup in the Agilent GC-FID, a system pressure of 5.0 psi was required to calibrate the helium flow through the preconcentrator and out the detector to a rate of 1.0 mL/min. Duplicate adsorption/thermal desorption test runs were conducted. Pure headspace vapors of hexane, 1,1,2,2-tetrachloroethane, and chlorobenzene were used. Vapor injections were made with a split inlet flow of 10:1, which meant that one tenth of the injected volume actually went through the preconcentrator. During each run, a blank heating was conducted before the injection of sample and subsequent desorption. From the duplicate runs, the average masses of pure VOCs adsorbed inside of the preconcentrator were calculated to be 24 ng for hexane, 318

ng for 1,1,2,2-tetrachloroethane, and 53 ng for chlorobenzene. Qualitatively, the duplicate hexane and chlorobenzene runs gave very similar results, and the tetrachloroethane runs gave moderately similar results. Not enough data points were collected for reasonable quantitative statistical analyses.

Figure 7 is an example chromatogram showing the adsorption/desorption profile obtained from the first hexane run. The first peak in Figure 7 was from the blank firing, the second peak was the breakthrough peak following hexane injection, and the third peak was the result of thermal desorption of analytes from the preconcentrator. The next three peaks were from the repeated hexane run, which also included a blank firing prior to hexane injection. Similar chromatograms were obtained for the 1,1,2,2-tetrachloroethane and chlorobenzene runs.

Both the breakthrough and desorption peaks for the hexane runs were clean and sharp with slight tailing. The chlorobenzene runs also gave clean, sharp peaks with some tailing. Figure 8 shows a chromatogram from the 1,1,2,2-tetrachloroethane runs. The breakthrough for both of the 1,1,2,2-tetrachloroethane runs showed up as a double peak, but the desorption peaks were clean and sharp. The double peak might have been due to the preconcentrator geometry or an interaction between the analyte and the uncoated preconcentrator surface or capillary tubing. Specifically, some of the analyte may have been condensing before reaching the detector. This double peak abnormality only showed up in the 1,1,2,2-tetrachloroethane runs, however, and more testing would need to be done to determine potential causes. Perhaps increasing the flow rate through the preconcentrator would have resulted in a single breakthrough peak instead.

Figure 7: Hexane adsorption/desorption chromatogram, duplicate 10:1 split runs for Precon #2

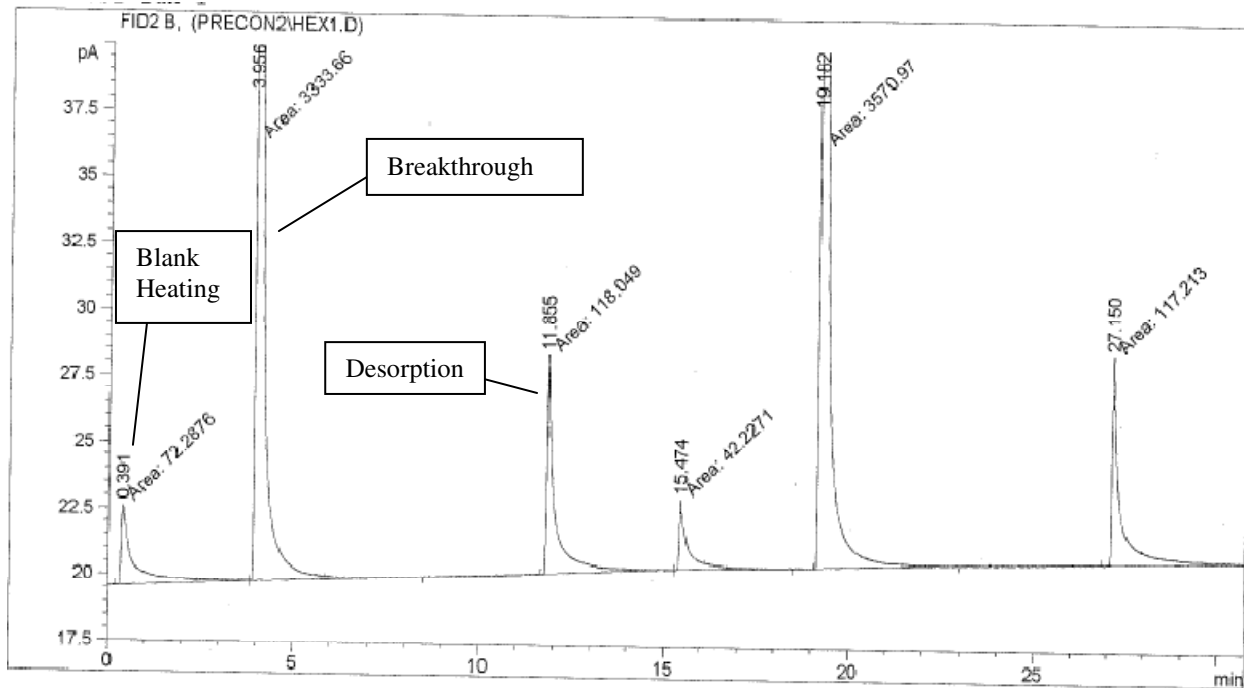
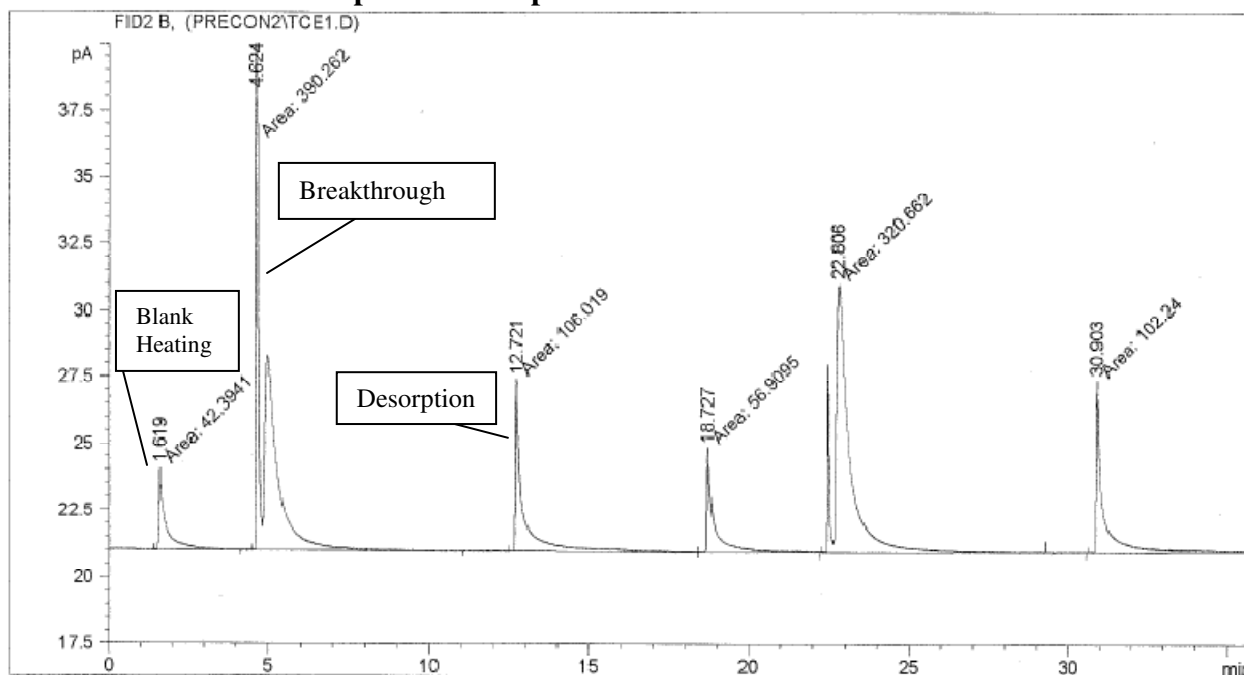


Figure 8: 1,1,2,2-tetrachloroethane adsorption/desorption chromatogram, duplicate 10:1 split runs for Precon #2



Tables 3-5 summarize the data obtained from all three of the duplicated VOC adsorption/desorption runs. The breakthrough area represented the integrated signal measurement of the breakthrough peak, the desorption area represented the integrated signal measurement of the thermal desorption peak. The total area represented the sum of the breakthrough area and the desorption area for a run. The percentage of analyte retained (% retained) was the percentage of the total area that the desorption peak represented, which was considered to be the fraction of analyte that was trapped or retained by the preconcentrator instead of breaking through during the adsorption phase of preconcentration. To calculate the amount of vapor injected, an ideal gas approximation was used: $n = PV/RT$, where n represents the amount in moles, P is the absolute pressure of the vapor, V represents the sample injection volume, R is the ideal gas constant, and T is the sample flask temperature. It was assumed that vapor pressure in the vented headspace was approximately 1 atm, and that vapor temperature was equal to the ambient temperature of approximately 293K. The injection volume was multiplied by the flow split ratio to represent the volume of sample vapor that actually went through the preconcentrator. The percentage of analyte retained was multiplied by the amount of analyte injected to determine the amount (in moles) of analyte adsorbed in the preconcentrator.

The following sample calculation demonstrates the determination of the moles of hexane adsorbed by the preconcentrator during the first hexane run shown in Table 3:

$$\begin{aligned} n &= PV * (\text{split flow ratio}) / (RT) \\ &= (1.0 \text{ atm})(2.0 \times 10^{-6} \text{ L})(1/10) / [(0.082057 \text{ L} \cdot \text{atm} \cdot \text{mol}^{-1} \cdot \text{K}^{-1})(293 \text{ K})] \\ &= 8.318 \times 10^{-9} \text{ mol} \end{aligned}$$

$$\% \text{ retained} = 100 * \text{desorbed area} / (\text{desorbed area} + \text{breakthrough area})$$

$$\begin{aligned}\text{Moles adsorbed} &= n * (\% \text{ retained}) / 100 \\ &= (8.179 \times 10^{-9} \text{ mol}) (3.42 / 100) = 2.84 \times 10^{-10} \text{ mol}\end{aligned}$$

The mass of analyte adsorbed was calculated as the product of the moles adsorbed and the molar mass of the analyte. The following sample calculation shows the mass adsorbed in the first hexane run shown in Table 3:

$$\begin{aligned}\text{Mass adsorbed} &= (\text{moles of hexane adsorbed}) * (\text{molar mass of hexane}) \\ &= (2.84 \times 10^{-10} \text{ mol}) (86.2 \text{ g/mol}) (10^9 \text{ ng/g}) = 25 \text{ ng}\end{aligned}$$

The same methods of calculation were used in Tables 4 and 5 for chlorobenzene and 1,1,2,2-tetrachloroethane. The molar masses used for chlorobenzene and 1,1,2,2-tetrachloroethane were 112.6 g/mol and 167.85 g/mol respectively.

The peaks from the blank heating were inconsistent but relatively substantial. It is possible that this is a reflection of active sites on the uncoated silicon being unable to desorb all of the trapped analyte in just one heating pulse. However, at this point it cannot be known whether or not these peaks were a function of VOCs, other compounds trapped and coming off of the preconcentrator, or slight decomposition of the capillary sealant because not very many blank heating runs were conducted before VOC testing was begun.

Additionally, Preconcentrator # 2 underwent testing before the 100:1 split runs were introduced. Due to time constraints, the 100:1 split runs were not run at a later time. Running vapors on this preconcentrator at a higher split flow, which would thus result in a lower amount of VOC vapor going through the preconcentrator, would perhaps give more insight into the double peak appearance.

Table 3: Hexane Adsorption/Desorption Results for Precon #2

<u>split</u>	<u>breakthrough area</u>	<u>desorption area</u>	<u>total area</u>	<u>% retained</u>	<u>moles adsorbed</u>	<u>mass (ng) adsorbed</u>
10:1	3333	118	3451	3.42	2.84E-10	25
10:1	3571	117	3688	3.17	2.64E-10	23

Table 4: Chlorobenzene Adsorption/Desorption Results for Precon #2

<u>split</u>	<u>breakthrough area</u>	<u>desorption area</u>	<u>total area</u>	<u>% retained</u>	<u>moles adsorbed</u>	<u>mass (ng) adsorbed</u>
10:1	1042	63.6	1106	5.75	4.79E-10	54
10:1	1118	64.5	1183	5.45	4.54E-10	51

Table 5: 1,1,2,2-Tetrachloroethane Adsorption/Desorption Results for Precon #2

<u>split</u>	<u>breakthrough area</u>	<u>desorption area</u>	<u>total area</u>	<u>% retained</u>	<u>moles adsorbed</u>	<u>mass (ng) adsorbed</u>
10:1	390	106	496	21.4	1.78E-09	298
10:1	320	102	422	24.2	2.01E-09	337

Preconcentrator #5: A system pressure of 3.7 psi was required to calibrate the air flow through preconcentrator #5 and out of the detector at a rate of 1.0 mL/min. Four adsorption/thermal desorption test runs conducted with 2.0 μ L vapor injections of chlorobenzene at a 10:1 split gave an average adsorbed mass of 425 ng. There was approximately 50% retention of analyte in the preconcentrator for these runs. Blank heating took place before the beginning of a new series of runs, but not between repeated runs. As a result, it is possible that the results of later runs in a series could have been skewed if there was not complete desorption of analytes from the preconcentrator with every run. Two chlorobenzene runs of 2.0 μ L vapor injection volumes at a 100:1 split gave an average adsorbed mass of 86 ng. The relative amount of analyte retained by the preconcentrator for these two runs was approximately 90%. In changing the split ration from 10:1 to 100:1, the volume of analyte flowing through the preconcentrator was decreased by a factor of ten. The observed increase in the percentage of analyte retained was expected as volume decreased to approach amounts of analyte below the breakthrough capacity threshold. The presence of breakthrough even at the 100:1 split might indicate that the volume required to reach the breakthrough capacity was lower than the volume of analyte that flowed through the preconcentrator at this split. It is plausible that the exposed surface area of the Tenax was not sufficient to trap all of the analyte at this split and injection volume.

Additionally, several additional injections of chlorobenzene were made at varying temperatures between 30°C and 70°C, but the resulting averaged peak areas fluctuated without showing any general trends.

Four adsorption/thermal desorption test runs conducted with 2.0 μL vapor injections of 1,1,2,2-tetrachloroethane at a 10:1 split gave an average adsorbed mass of 811 ng, and two runs at a 100:1 split gave an average adsorbed mass of 140 ng. The percentage of analyte retained was approximately 60% at the 10:1 split and 100% at the 100:1 split. The 100% retention resulted from the absence of a breakthrough peak for those runs, which indicated that the total amount of analyte flowing into the preconcentrator was below the breakthrough capacity.

The chromatograms in Figures 9 and 10 show some of the adsorption/desorption profiles obtained from chlorobenzene runs at 10:1 and 100:1 split flows, respectively. Blank heating was not conducted between runs in a continuous series, and the blank heatings that were conducted prior to starting each series were not included in the recorded chromatograms.

When present, the breakthrough peaks for all chlorobenzene and 1,1,2,2-tetrachloroethane runs were sharp but showed some tailing. This may be due to oversaturation of the trap, resulting in slow removal of excess analyte due to intermolecular attraction rather than sorption interactions with the Tenax. The desorption peaks for all runs, even the 1,1,2,2-tetrachloroethane runs with no breakthrough, were not very symmetric and showed a combination of tailing and a broad but short double peak. This may be due to re-adsorption on the capillary connection transfer line between the preconcentrator and the detector. The lack of a defined and even desorption peak perhaps compromises strict quantitative analysis, but the calculated analyte retentions might still be useful when taken as approximations.

Tables 6 and 7 show the data from the chlorobenzene and 1,1,2,2-tetrachloroethane adsorption/desorption runs. Due to a melted seal attaching the preconcentrator to one of the capillary connectors, preconcentrator #5 was rendered nonoperational before hexane vapor runs were conducted.

Two-component (chlorobenzene/1,1,2,2-tetrachloroethane) and ten-component (VOC mix) mixed vapor flasks were prepared. Figures 11 and 12 show the resulting chromatograms from 2.0 μL vapor injections at 10:1 splits. In both cases, the mixes came out as a single narrow peak with some tailing, implying that transfer of a mix of compounds from the preconcentrator to a column for separation was feasible.

Figure 9: Chlorobenzene adsorption/desorption chromatogram, duplicate 10:1 split runs for Precon #5

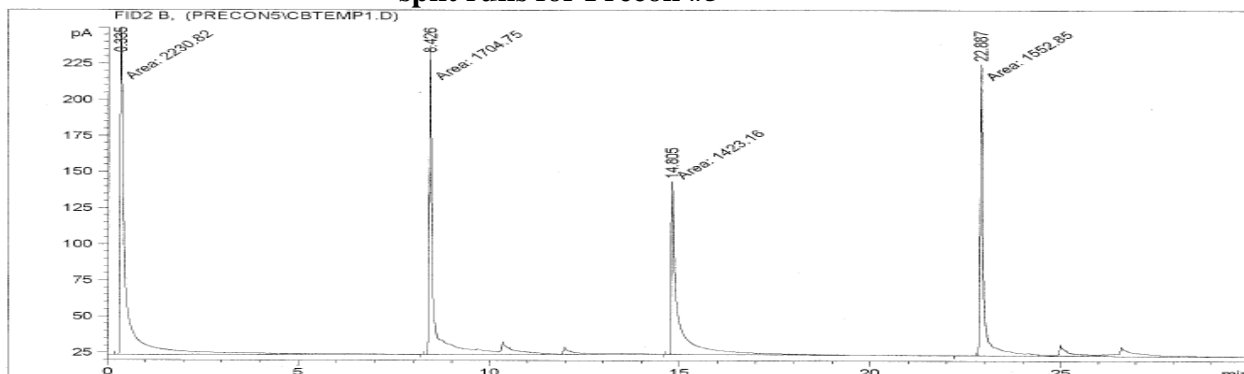


Figure 10: Chlorobenzene adsorption/desorption chromatogram, duplicate 100:1 split runs for Precon #5

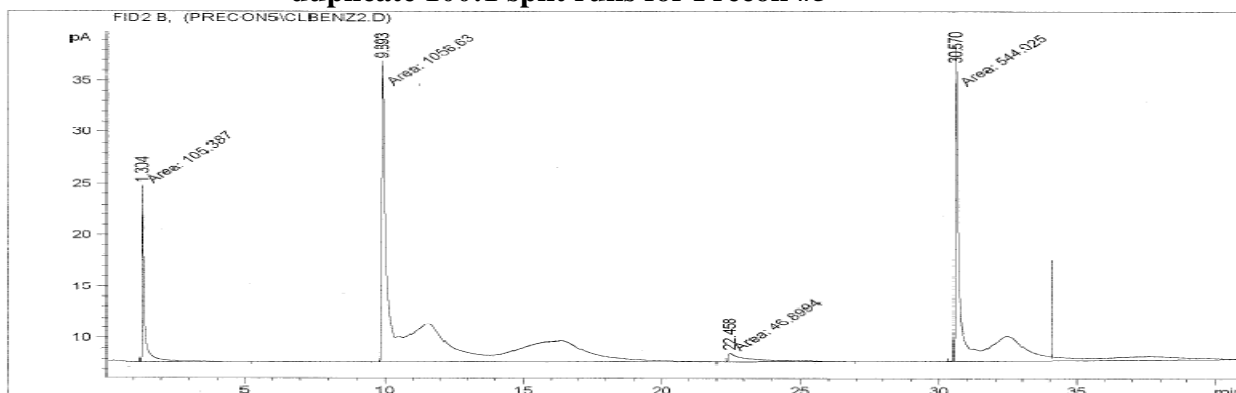


Table 6: Chlorobenzene Adsorption/Desorption Results for Precon #5

<u>split</u>	<u>breakthrough area</u>	<u>desorption area</u>	<u>total area</u>	<u>% on precon</u>	<u>moles adsorbed</u>	<u>mass (ng) adsorbed</u>
10:1	1862	1156	3018	38.3	3.19E-09	359
10:1	1196	1086	2282	47.6	3.96E-09	446
10:1	2231	1705	3936	43.3	3.60E-09	406
10:1	1423	1553	2976	52.2	4.34E-09	489
100:1	105.4	1057	1162	90.9	7.56E-10	85
100:1	46.9	544	590.9	92.1	7.66E-10	86

Table 7: 1,1,2,2-Tetrachloroethane Adsorption/Desorption Results for Precon #5

<u>split</u>	<u>breakthrough area</u>	<u>desorption area</u>	<u>total area</u>	<u>% on precon</u>	<u>moles adsorbed</u>	<u>mass (ng) adsorbed</u>
10:1	502	988	1490	66.3	5.52E-09	926
10:1	611	501	1112	45.1	3.75E-09	629
10:1	393	471	864	54.5	4.53E-09	761
10:1	494	984	1478	66.6	5.54E-09	930
100:1	0	287	287	100	8.32E-10	140
100:1	0	292	292	100	8.32E-10	140

Figure 11: Chromatogram from chlorbenzene and 1,1,2,2-tetrachloroethane mix, 10:1 split for Precon #5

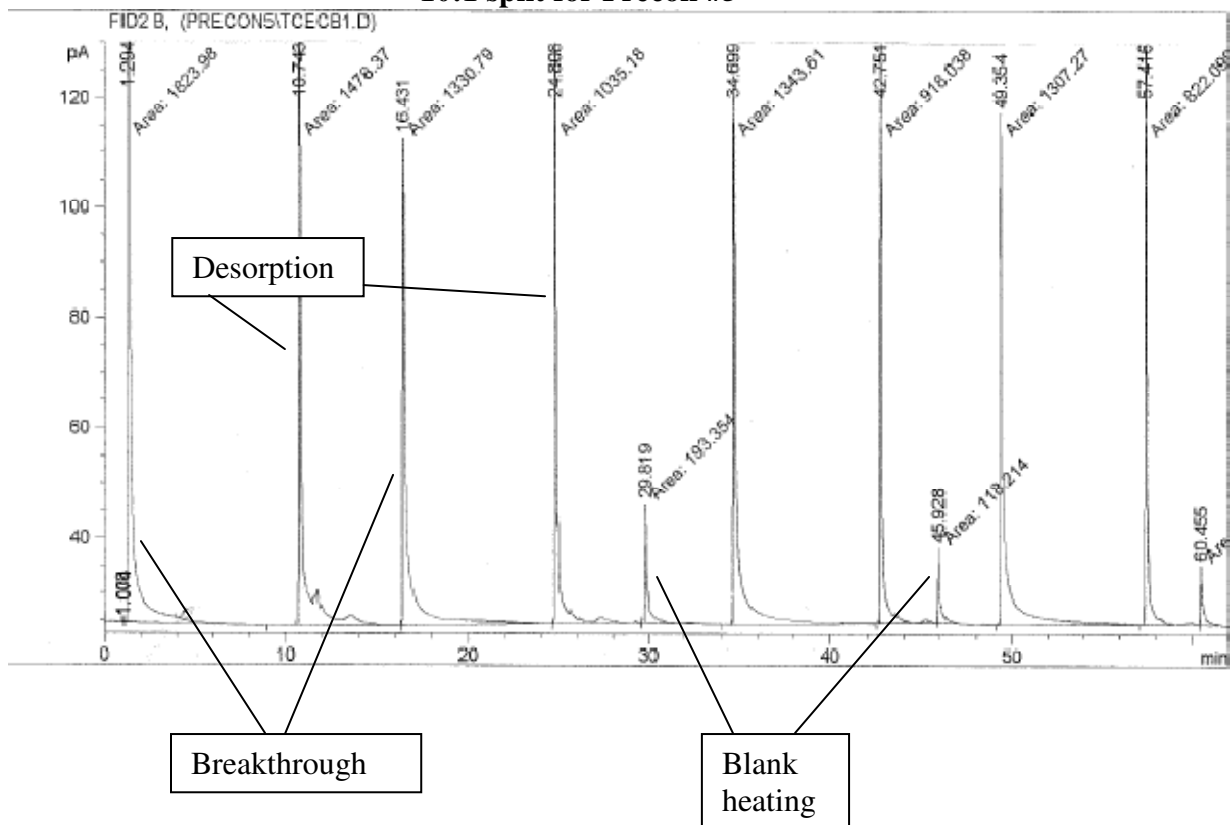
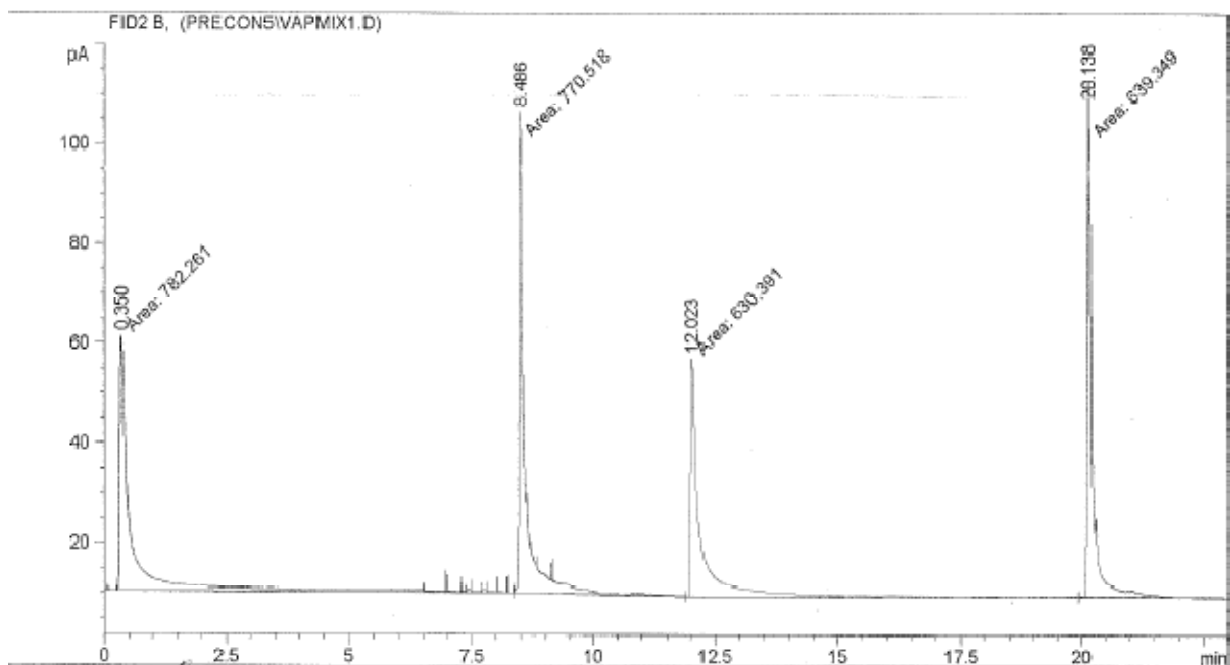


Figure 12: Chromatogram from 10-component VOC mix, 10:1 split for Precon #5



Preconcentrator #6: A system pressure of 3.3 psi was required to calibrate the system gas flow to 1.0 mL/min with the preconcentrator installed. Two adsorption/thermal desorption runs of 2.0 μ L vapor injections of hexane at a 10:1 split gave an average adsorbed mass of 31 ng, and two more runs at a 100:1 split gave an average adsorbed mass of 7 ng, which corresponded to approximately analyte retention of 4% and 10% for the 10:1 split and 100:1 split runs respectively. The obtained analyte adsorption values were quite reproducible from one run to the next at both flow split levels. Blank heating took place before the beginning of a new series of runs, but there was no blank heating between the first run and the repeated run at a given split. Hexane breakthrough peaks were sharp with some tailing at both splits. The desorption runs were sharp with noisy tailing at the 10:1 split and fairly broad and asymmetric at the 100:1 split, as seen in the chromatograms shown in Figures 13 and 14.

Two chlorobenzene runs of 2.0 μ L vapor injection volumes at a 10:1 split gave an average adsorbed mass of 371 ng, which corresponded to a retention of approximately 40%, and two more runs at a 100:1 split gave an average adsorbed mass of 62 ng, which corresponded to a retention of approximately 62%. The chlorobenzene peaks showed breakthrough peaks with substantial tailing. This may have been caused by temporary multi-layer analyte adsorption due to nonbonding interactions such as the Van der Waals force. If so, the layers beyond the monolayer of analytes directly interacting with the Tenax sorbent would be slowly driven off by the carrier gas flow, which would account for the long peak tails. The desorption peaks, however, were much sharper and only showed slight tailing. Figure 15 shows a representative chromatogram from a series of 100:1 split runs.

Three adsorption/thermal desorption test runs conducted with 2.0 μL vapor injections of 1,1,2,2-tetrachloroethane at a 10:1 split gave an average adsorbed mass of 417 ng, and two runs at a 100:1 split gave an average adsorbed mass of 114 ng. The percentage of analyte retained was approximately 30% at the 10:1 split and 82% at the 100:1 split. The breakthrough showed irregular double peaks and substantial tailing. Again, this could have been the result of multi-layer adsorption due to overloading the preconcentrator with analyte. The desorption peaks were sharp but slightly noisy. Figure 16 shows a chromatogram with 10:1 split runs and demonstrates the irregular double peaks for which quantization was likely compromised.

For all compounds, the presence of breakthrough peaks even at the 100:1 split implies that breakthrough capacity was lower than the amount of analyte that flowed through the preconcentrator at this split. Perhaps the post spacing and geometry of the preconcentrator were such that the analyte flow through the preconcentrator did not come into sufficient contact with the Tenax coating on all surfaces of the preconcentrator or that insufficient adsorbent was available even at these low amounts of analytes. Tables 8-10 show collected adsorption/desorption data for all three compounds.

Figure 13: Hexane Adsorption/Desorption Profile, 10:1 split runs for Precon #6

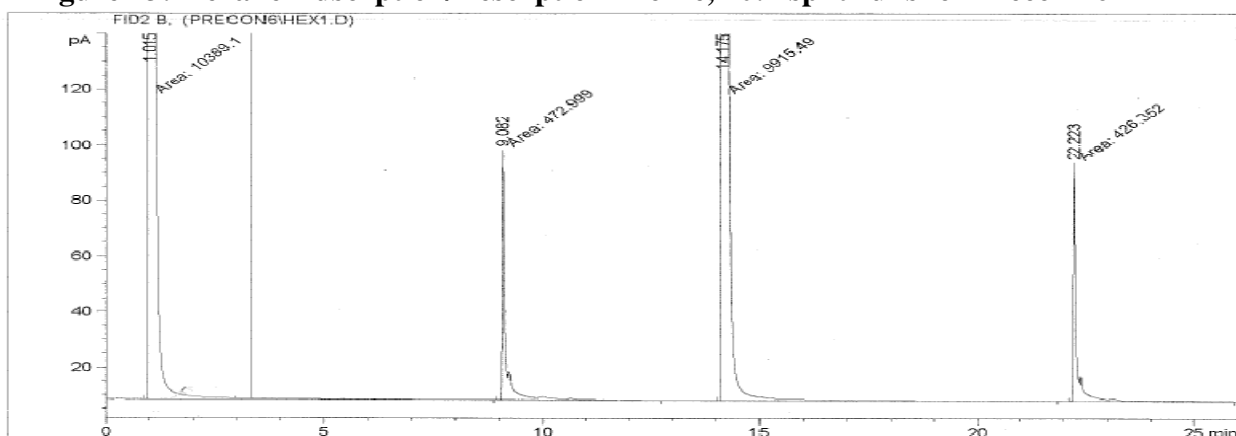


Figure 14: Hexane Adsorption/Desorption Profile, 100:1 split runs for Precon #6

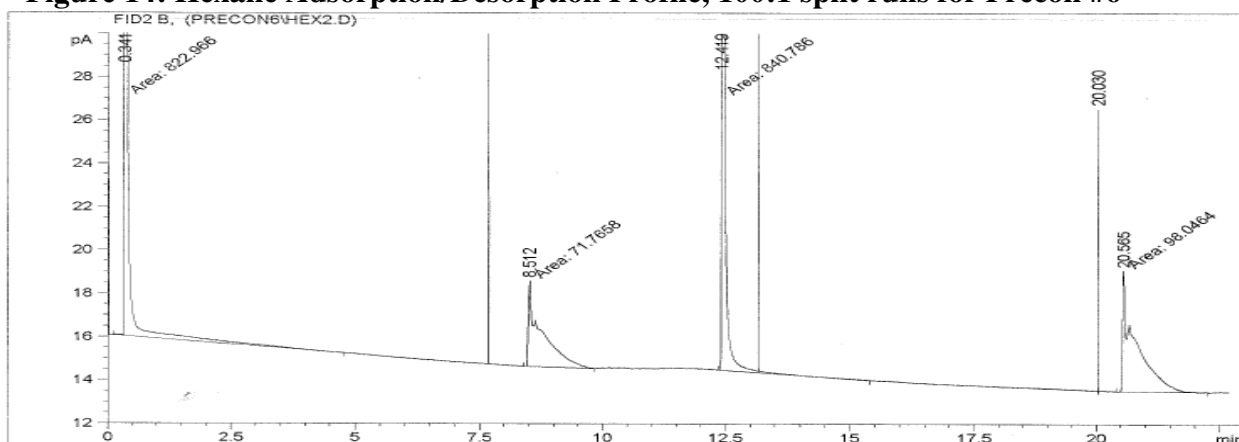


Figure 15: Chlorobenzene Adsorption/Desorption Profile, 100:1 split runs for Precon #6

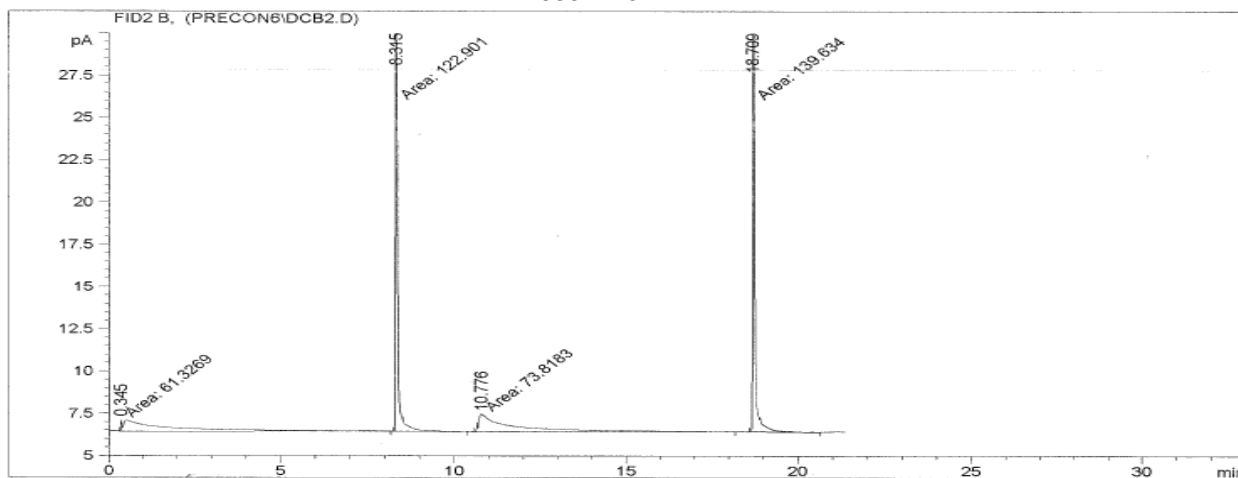


Figure 16: 1,1,2,2-Tetrachloroethane Adsorption/Desorption Profile, 10:1 split runs for Precon #6

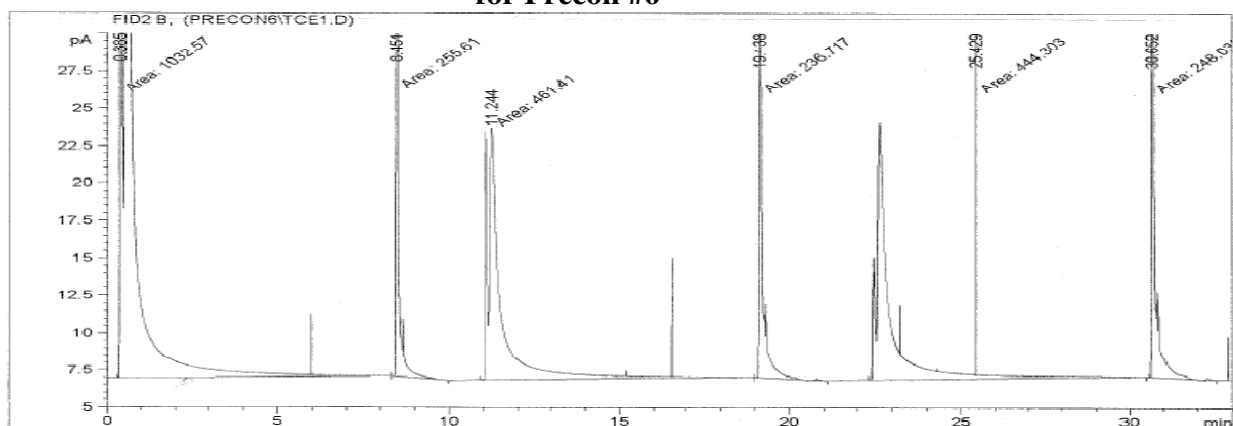


Table 8: Hexane Adsorption/Desorption Results for Precon #6

<u>split</u>	<u>breakthrough area</u>	<u>desorption area</u>	<u>total area</u>	<u>% retained</u>	<u>moles adsorbed</u>	<u>mass (ng) adsorbed</u>
10:1	10390	473	10863	4.35	3.62E-10	31
10:1	9915	426.4	10341.4	4.12	3.43E-10	30
100:1	823	71.76	894.76	8.02	6.67E-11	6
100:1	840.8	98.05	938.85	10.4	8.69E-11	7

Table 9: 1,1,2,2-Tetrachloroethane Adsorption/Desorption Results for Precon #6

<u>split</u>	<u>breakthrough area</u>	<u>desorption area</u>	<u>total area</u>	<u>% retained</u>	<u>moles adsorbed</u>	<u>mass (ng) adsorbed</u>
10:1	1033	255.6	1288.6	19.8	1.65E-09	277
10:1	461.4	236.7	698.1	33.9	2.82E-09	473
10:1	444.3	248	692.3	35.8	2.98E-09	500
100:1	25.3	127.2	152.5	83.4	6.94E-10	116
100:1	26.82	108.6	135.42	80.2	6.67E-10	112

Table 10: Chlorobenzene Adsorption/Desorption Results for Precon #6

<u>split</u>	<u>breakthrough area</u>	<u>desorption area</u>	<u>total area</u>	<u>% retained</u>	<u>moles adsorbed</u>	<u>mass (ng) adsorbed</u>
10:1	1038	735.3	1773.3	41.5	3.45E-09	388
10:1	1226	747.5	1973.5	37.9	3.15E-09	355
100:1	61.33	122.9	184.23	66.7	5.55E-10	62
100:1	73.82	139.6	213.42	65.4	5.44E-10	61

Preconcentrator #8: A system pressure of 6.5 psi was needed to reach a flow rate of 1.0 mL/min through the GC system with preconcentrator #8 installed. Six adsorption/thermal desorption test runs conducted with 2.0 μ L vapor injections of chlorobenzene at a 10:1 split gave an average adsorbed mass of 554 ng, and three runs at a 100:1 split gave an average adsorbed mass of 60 ng. There was approximately 60% retention of analyte in the preconcentrator for the 10:1 split runs and 65% analyte retention for the 100:1 split runs. Blank heating of the preconcentrator was conducted at the beginning of a new series of runs but not between repeated runs. Figure 17 shows a chromatogram of the 10:1 split runs.

Breakthrough peaks from the 100:1 split runs imply that even with the low volume of analyte used, the preconcentrator was saturated. Lower volumes might show less if any breakthrough. However, there was only a 5% change in analyte retention with a split flow ratio by an order of magnitude. For such similar retention percentages with a change of 10 times the volume injected onto the preconcentrator, it is implied that variables other than injection amount might be in question. For example, the design of the preconcentrator might not have allowed the analyte flowing through the preconcentrator to come into sufficient contact with the Tenax surface coating.

Four adsorption/thermal desorption test runs conducted with 2.0 μ L vapor injections of 1,1,2,2-tetrachloroethane at a 10:1 split gave an average adsorbed mass of 616 ng, and three runs at a 100:1 split gave an average adsorbed mass of 140 ng. The percentage of analyte retained was approximately 45% at the 10:1 split and 100% at the 100:1 split. The 100% retention resulted from the absence of a breakthrough peak, implying that the total amount of analyte flowing onto the preconcentrator was below the

breakthrough capacity and thus completely adsorbed. Figure 18 shows a chromatogram of 10:1 split runs of 1,1,2,2-tetrachloroethane.

Figure 17: Chlorobenzene adsorption/desorption chromatogram, triplicate 10:1 split runs for Precon #8

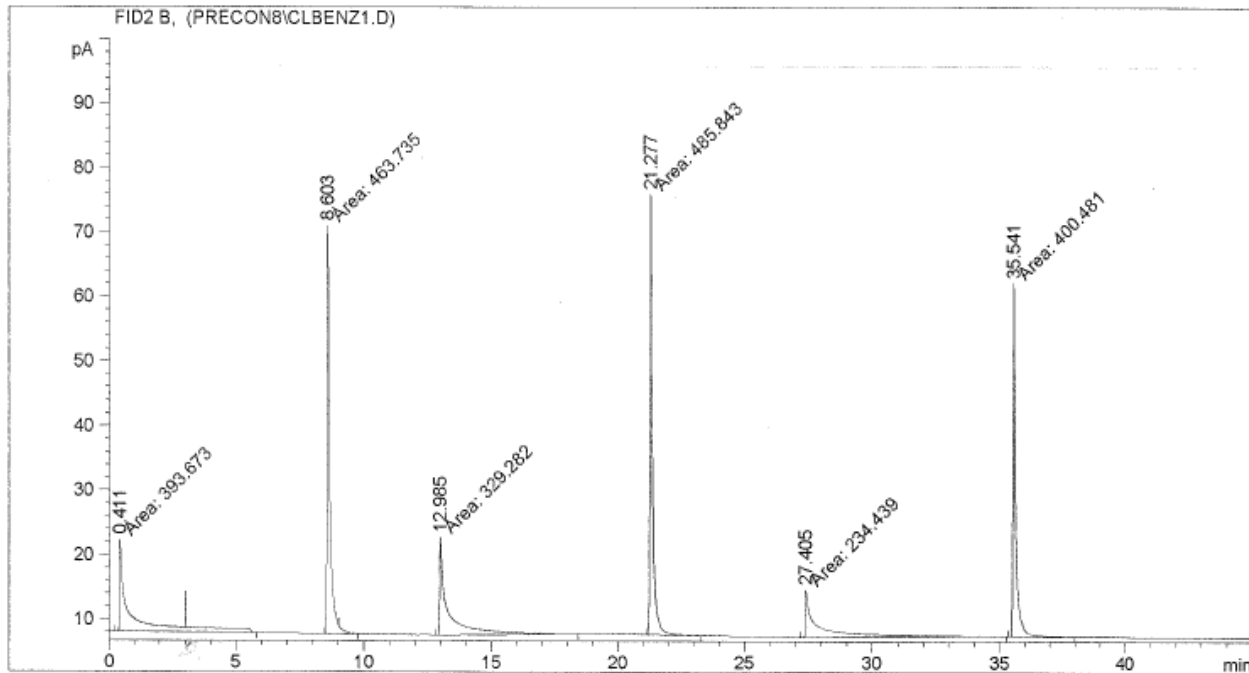


Figure 18: 1,1,2,2-Tetrachloroethane adsorption/desorption chromatogram, triplicate 10:1 split runs for Precon #8

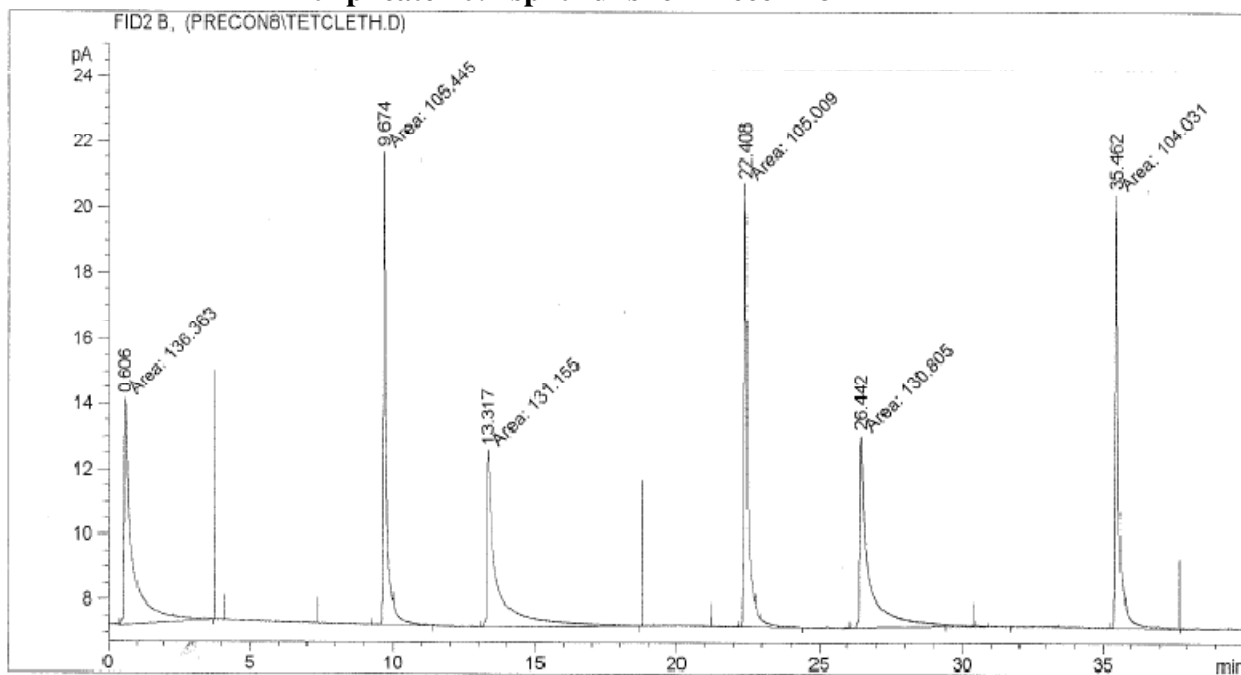


Table 11: Chlorobenzene Adsorption/Desorption Results for Precon #8

<u>split</u>	<u>breakthrough area</u>	<u>desorption area</u>	<u>total area</u>	<u>% retained</u>	<u>moles adsorbed</u>	<u>mass (ng) adsorbed</u>
10:1	393.7	463.7	857.4	54.1	4.50E-09	507
10:1	329.3	485.8	815.1	59.6	4.96E-09	558
10:1	234.4	400.5	634.9	63.1	5.25E-09	591
10:1	312.7	416.6	729.3	57.1	4.75E-09	535
10:1	200.8	328.5	529.3	62.1	5.16E-09	581
10:1	261.6	376.8	638.4	59.0	4.91E-09	553
100:1	43.34	312.9	356.24	87.8	7.31E-10	82
100:1	82.42	106.1	188.52	56.3	4.68E-10	53
100:1	85.87	83.02	168.89	49.2	4.09E-10	46

Table 12: 1,1,2,2-Tetrachloroethane Adsorption/Desorption Results for Precon #8

<u>split</u>	<u>breakthrough area</u>	<u>desorption area</u>	<u>total area</u>	<u>% retained</u>	<u>moles adsorbed</u>	<u>mass (ng) adsorbed</u>
10:1	136.4	105.4	241.8	43.6	3.63E-09	609
10:1	131.2	105	236.2	44.5	3.70E-09	621
10:1	130.8	104	234.8	44.3	3.68E-09	618
100:1	0	29.9	29.9	100	8.32E-10	140
100:1	0	20.7	20.7	100	8.32E-10	140
100:1	0	23.4	23.4	100	8.32E-10	140

Preconcentrator #9: To calibrate flow to 1.0 mL/min through the setup when preconcentrator #9 was installed, a system pressure of 3.0 psi was required. Blank heating took place before the beginning of a new series of runs, but not always between repeated runs. There may not have been complete desorption between runs because of the continuous running without blank heating. Two adsorption/thermal desorption test runs conducted with 2.0 μ L vapor injections of hexane at a 10:1 split gave an average adsorbed mass of 36 ng, and three runs at a 100:1 split gave an average adsorbed mass of 16 ng. There was approximately 5% retention of hexane in the preconcentrator for the 10:1 split runs and 23% retention for the 100:1 split runs.

Two chlorobenzene runs of 2.0 μ L vapor injection volumes at a 10:1 split gave an average adsorbed mass of 86 ng, and two runs at a 100:1 split gave an average adsorbed mass of 42 ng. The relative amount of analyte retained by the preconcentrator for the two 10:1 split runs was approximately 20% and for the two 100:1 splits was 45%. The presence of breakthrough even at the 100:1 split indicates that the volume required to reach the breakthrough capacity was lower than the volume of analyte that flowed through the preconcentrator at this split. Alternatively, perhaps the post spacing and geometry of the preconcentrator were such that analyte flowing through the preconcentrator did not come into sufficient contact with all surfaces of the Tenax coating inside the preconcentrator.

Two adsorption/thermal desorption test runs conducted with 2.0 μ L vapor injections of 1,1,2,2-tetrachloroethane at a 10:1 split gave an average adsorbed mass of 337 ng, and two runs at a 100:1 split gave an average adsorbed mass of 91 ng. The

percentage of analyte retained was approximately 24% at the 10:1 split and 65% at the 100:1 split.

Figures 19-22 show chlorobenzene and 1,1,2,2-tetrachloroethane runs at 10:1 and 100:1 splits, and Tables 13-15 show adsorption/desorption data for all three compounds. The chlorobenzene breakthrough peaks were sharp with slight tailing. The desorption peaks for the 10:1 splits were sharp and clean, and the desorption peaks for the 100:1 splits were sharp but with slightly noisy tailing. The 1,1,2,2-tetrachloroethane breakthrough peaks were sharp with moderate tailing. The desorption peaks were irregularly shaped, which compromised the quantitative integration of peak areas.

Qualitatively, all of the runs except for the hexane 100:1 splits seemed to be moderately repeatable with respect to peak size, shape, and relative area.

Figure 19: Chlorobenzene adsorption/desorption chromatogram, triplicate 10:1 split runs for Precon #9

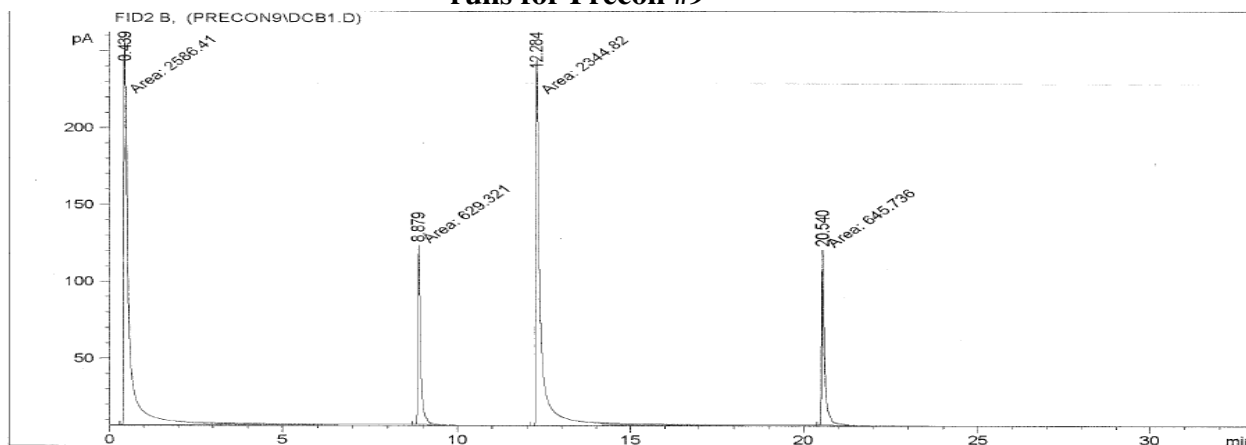


Figure 20: Chlorobenzene adsorption/desorption chromatogram, triplicate 100:1 split runs for Precon #9

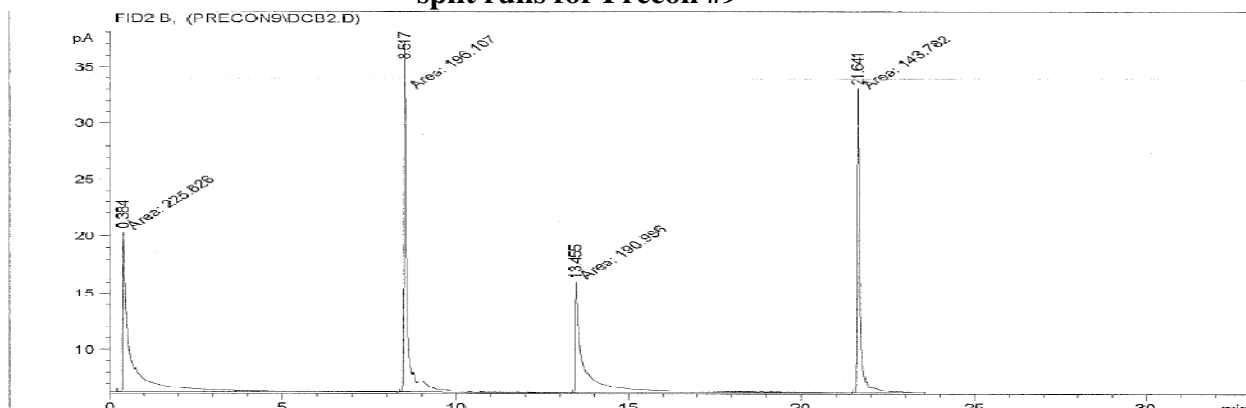


Figure 21: 1,1,2,2-Tetrachloroethane adsorption/desorption chromatogram, duplicate 10:1 split runs for Precon #9

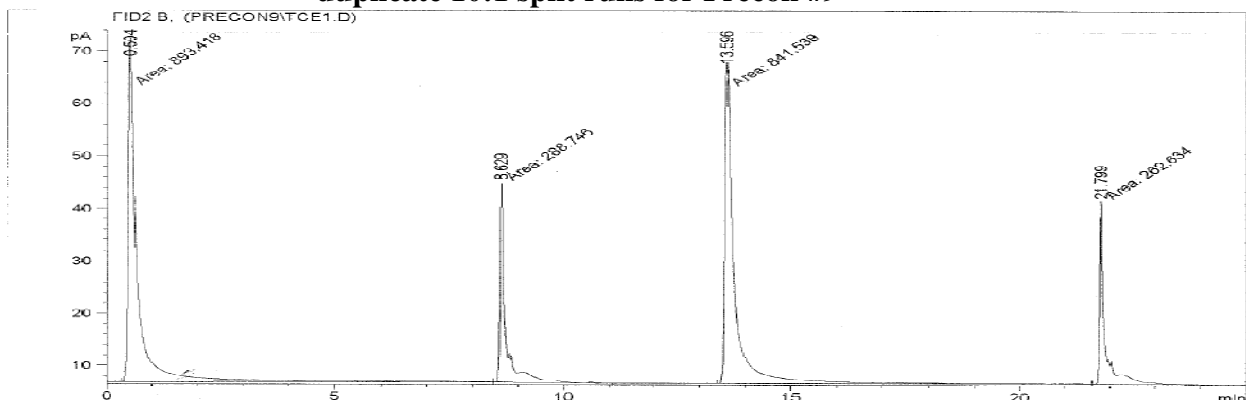


Figure 22: 1,1,2,2-Tetrachloroethane adsorption/desorption chromatogram, duplicate 100:1 split runs for Precon #9

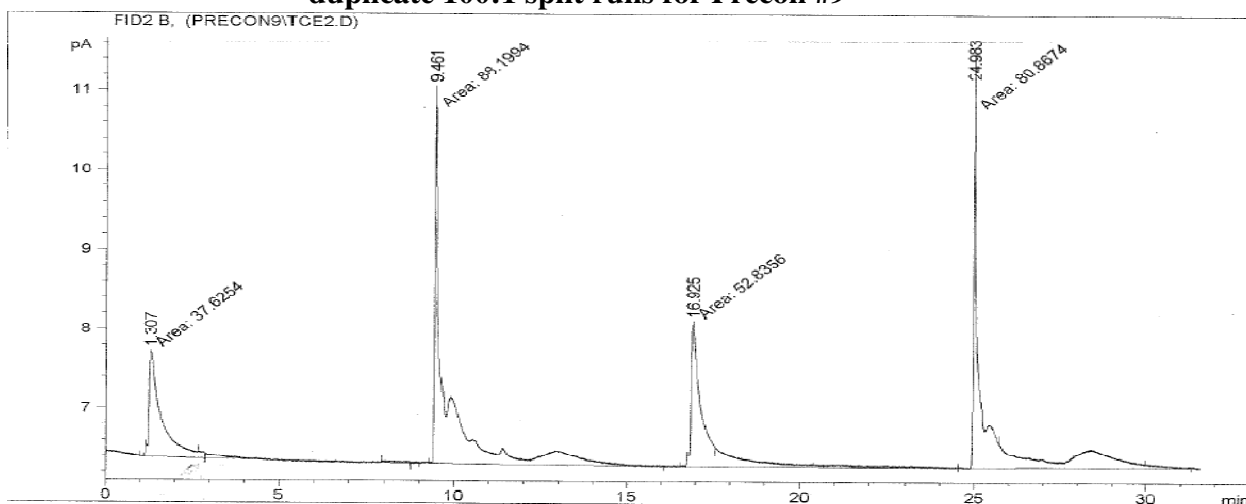


Table 13: Hexane Adsorption/Desorption Results for Precon #9

<u>split</u>	<u>breakthrough area</u>	<u>desorption area</u>	<u>total area</u>	<u>% retained</u>	<u>moles adsorbed</u>	<u>mass (ng) adsorbed</u>
10:1	8280	437	8717	5.01	4.17E-10	36
10:1	8410	449.4	8859.4	5.07	4.22E-10	36
100:1	767.4	479.2	1246.6	38.4	3.20E-10	28
100:1	833.3	179.5	1012.8	17.7	1.47E-10	13
100:1	801	110.4	911.4	12.1	1.01E-10	9

Table 14: Chlorobenzene Adsorption/Desorption Results for Precon #9

<u>split</u>	<u>breakthrough area</u>	<u>desorption area</u>	<u>total area</u>	<u>% retained</u>	<u>moles adsorbed</u>	<u>mass (ng) adsorbed</u>
10:1	2586	629.3	3215.3	19.6	1.63E-09	183
10:1	2345	645.7	2990.7	21.6	1.80E-09	202
100:1	225.6	196.1	421.7	46.5	3.87E-10	44
100:1	191	143.8	334.8	43.0	3.57E-10	40

Table 15: 1,1,2,2-Tetrachloroethane Adsorption/Desorption Results for Precon #9

<u>split</u>	<u>breakthrough area</u>	<u>desorption area</u>	<u>total area</u>	<u>% retained</u>	<u>moles adsorbed</u>	<u>mass (ng) adsorbed</u>
10:1	893.4	288.7	1182.1	24.4	2.03E-09	341
10:1	841.5	262.6	1104.1	23.8	1.98E-09	332
100:1	37.62	88.20	125.82	70.1	5.83E-10	98
100:1	52.84	80.87	133.71	60.5	5.03E-10	84

Preconcentrator #11: A system pressure of 3.0 psi was required to calibrate the GC flow to 1.0 mL/min when preconcentrator #11 was installed. Blank heating runs were conducted at the beginning of a new series of runs, but not always between repeated runs. Five adsorption/thermal desorption test runs were conducted with 2.0 μ L vapor injections of hexane at a 10:1 split gave an average adsorbed mass of 84 ng, and six runs were conducted at 100:1 splits to give an average desorbed mass of 9 ng. For the 10:1 split runs, there was approximately 12% retention of hexane in the preconcentrator, and for the 100:1 split runs there was approximately 13% retention of hexane. The similar retention percentages might imply overloading at the volumes used, but perhaps other variables might be influencing the interaction of analyte with the polymeric surface coating. Figure 23 shows a chromatogram for a 10:1 split run. The hexane peaks were smooth and sharp with some tailing on the breakthrough peaks most likely due to preconcentrator overloading.

Two chlorobenzene runs of 2.0 μ L vapor injection volumes at a 10:1 split gave an average adsorbed mass of 916 ng, and three runs at a 100:1 split gave an average adsorbed mass of 94 ng. The relative amount of analyte retained by the preconcentrator for the two 10:1 split runs was approximately 98% and for the two 100:1 splits was 100%. Figure 24 shows chlorobenzene runs at a 10:1 split. The breakthrough peaks were very small, and the desorption peaks were sharp and narrow, which is ideal for analytical purposes. Figure 25 shows 100:1 split runs of chlorobenzene. There were no breakthrough peaks, and the desorption peaks were sharp but had an irregularity near the baseline.

Two adsorption/thermal desorption test runs conducted with 2.0 μL vapor injections of 1,1,2,2-tetrachloroethane at a 10:1 split gave an average adsorbed mass of 1396 ng, and the percentage of analyte retained was 100%. Since the 10:1 split runs were presumed to be of a low enough amount of analyte that no breakthrough appeared, the 100:1 splits of chlorobenzene were not run at the same time. Figure 6 shows a chromatogram for the 10:1 split runs. Tables 16-18 show adsorption/desorption data for all three compounds.

Figure 23: Hexane Adsorption/Desorption Profile, 10:1 split runs for Precon #11

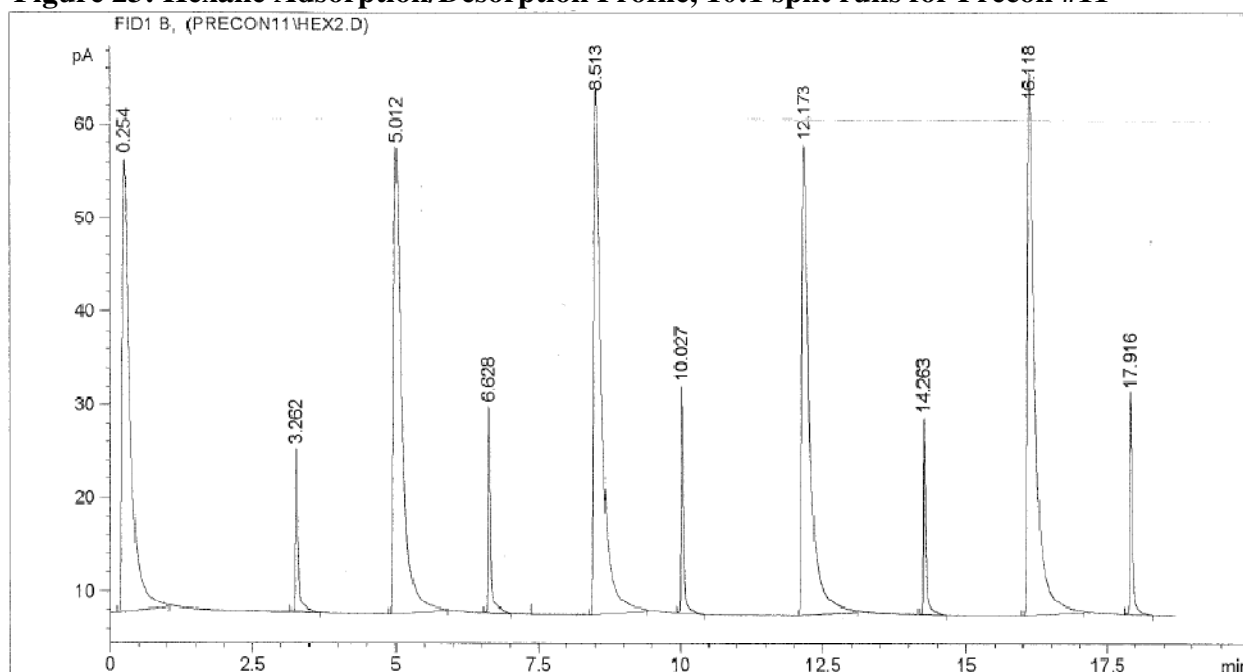


Figure 24: Chlorobenzene adsorption/desorption chromatogram, 10:1 split runs for Precon #11

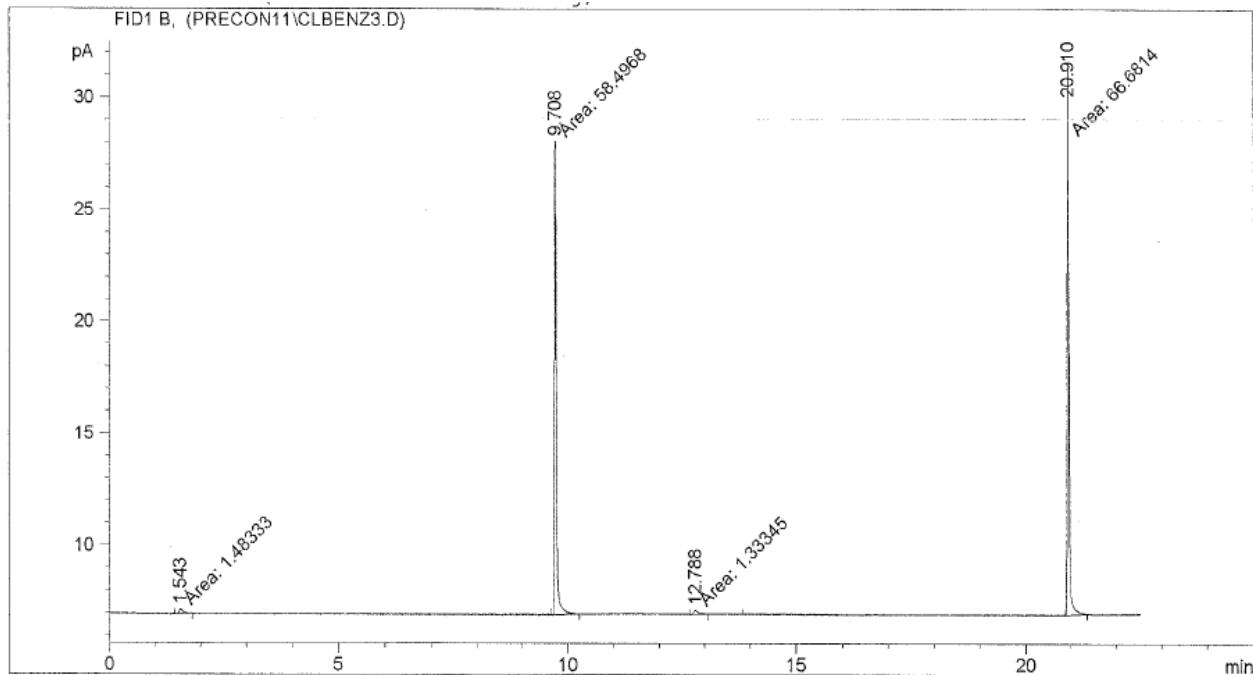
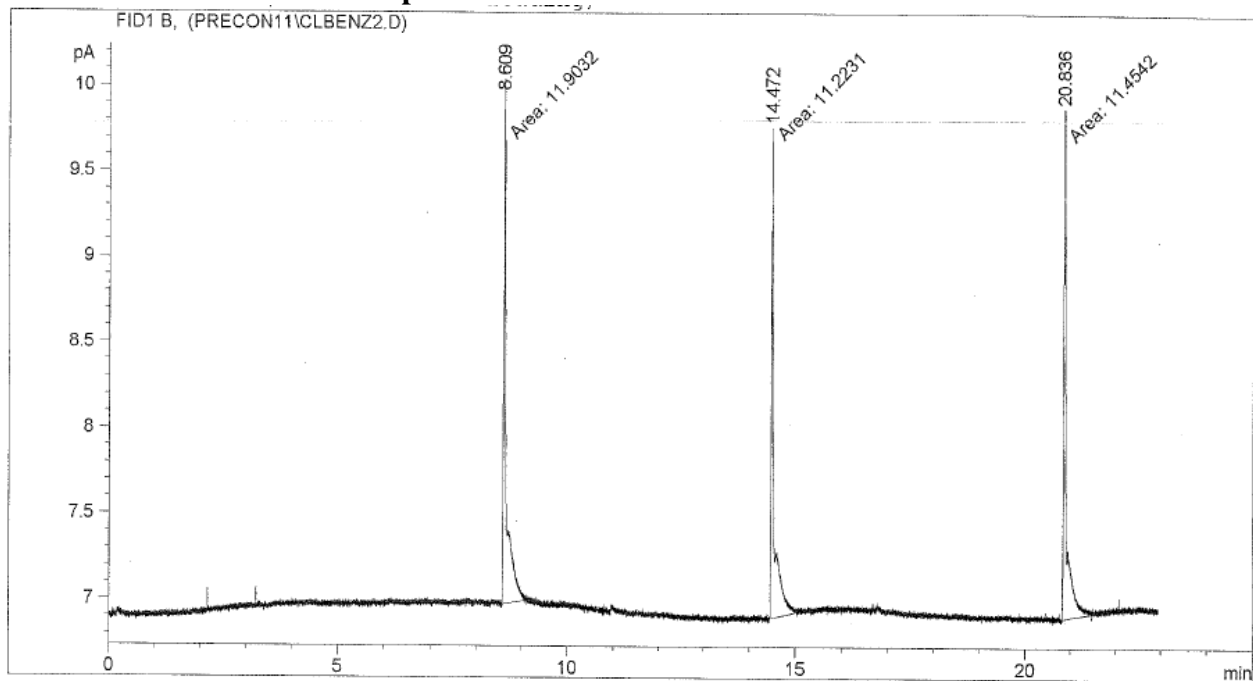


Figure 25: Chlorobenzene adsorption/desorption chromatogram, 100:1 split runs for Precon #11



**Figure 26: 1,1,2,2-Tetrachloroethane adsorption/desorption chromatogram,
10:1 split runs for Precon #11**

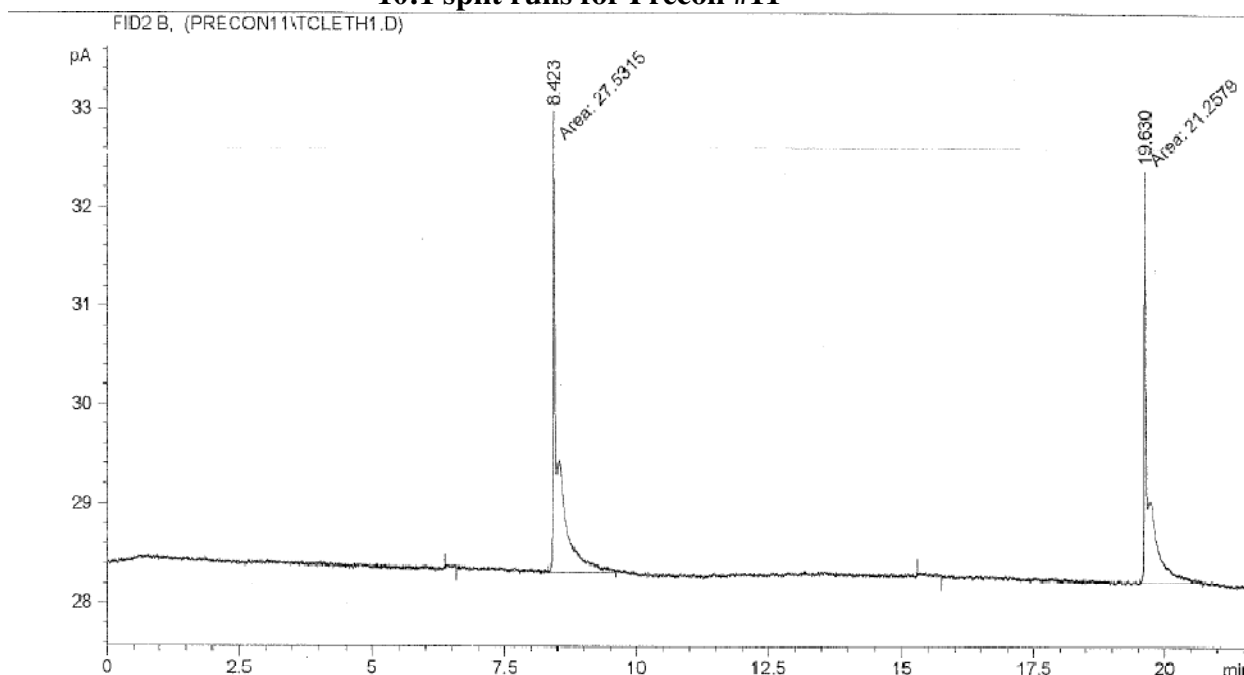


Table 16: Hexane Adsorption/Desorption Results for Precon #11

<u>split</u>	<u>breakthrough</u> <u>area</u>	<u>desorption</u> <u>area</u>	<u>total</u> <u>area</u>	<u>%</u> <u>retained</u>	<u>moles</u> <u>adsorbed</u>	<u>mass</u> <u>(ng)</u> <u>adsorbed</u>
10:1	496	59.8	555.8	10.8	8.95E-10	77
10:1	491	70.8	561.8	12.6	1.05E-09	90
10:1	563	76.1	639.1	11.9	9.91E-10	85
10:1	505	66.9	571.9	11.7	9.73E-10	84
10:1	578	76.1	654.1	11.6	9.68E-10	83
100:1	52.4	8.11	60.51	13.4	1.11E-10	10
100:1	54.2	8.09	62.29	13.0	1.08E-10	9
100:1	49.9	8.15	58.05	14.0	1.17E-10	10
100:1	54	8.04	62.04	13.0	1.08E-10	9
100:1	65.8	8.52	74.32	11.5	9.54E-11	8
100:1	61.6	7.95	69.55	11.4	9.51E-11	8

Table 17: Chlorobenzene Adsorption/Desorption Results for Precon #11

<u>split</u>	<u>breakthrough area</u>	<u>desorption area</u>	<u>total area</u>	<u>% retained</u>	<u>moles adsorbed</u>	<u>mass (ng) adsorbed</u>
10:1	1.48	58.5	59.98	97.5	8.11E-09	914
10:1	1.33	66.7	68.03	98.0	8.16E-09	918
100:1	0	11.9	11.9	100	8.32E-10	94
100:1	0	11.2	11.2	100	8.32E-10	94
100:1	0	11.5	11.5	100	8.32E-10	94

Table 18: 1,1,2,2-Tetrachloroethane Adsorption/Desorption Results for Precon #11

<u>split</u>	<u>breakthrough area</u>	<u>desorption area</u>	<u>total area</u>	<u>% retained</u>	<u>moles adsorbed</u>	<u>mass (ng) adsorbed</u>
10:1	0	27.53	27.53	100	8.32E-09	1396
10:1	0	21.26	21.26	100	8.32E-09	1396

Another experiment was conducted in which the system pressure was changed. 2.0 μ L vapor injections of hexane were used at a 10:1 split. Figure 27 shows a graph of the average retention percentages at various pressures. Most likely, an increased flow would not allow for sufficient equilibration between the analyte and the Tenax adsorbent.

A later experiment showed that the desorption area decreased slightly with time between injection and desorption until approximately 8 minutes. Hexane was also used for this experiment, and the flow was set to a 10:1 split. Figure 28 is a graph of the results showing that after about 8 minutes, the area leveled off. This may indicate that some of the initial amount of “adsorbed” analyte was not actually adsorbed on the Tenax, but instead was slowly removed from multiple layers of analyte on the Tenax surface.

Preconcentrator #11 developed a crack in the Pyrex top plate and became nonoperational before other tests were run.

Figure 27: Pressure variation experiment, hexane 10:1 splits for Precon #11

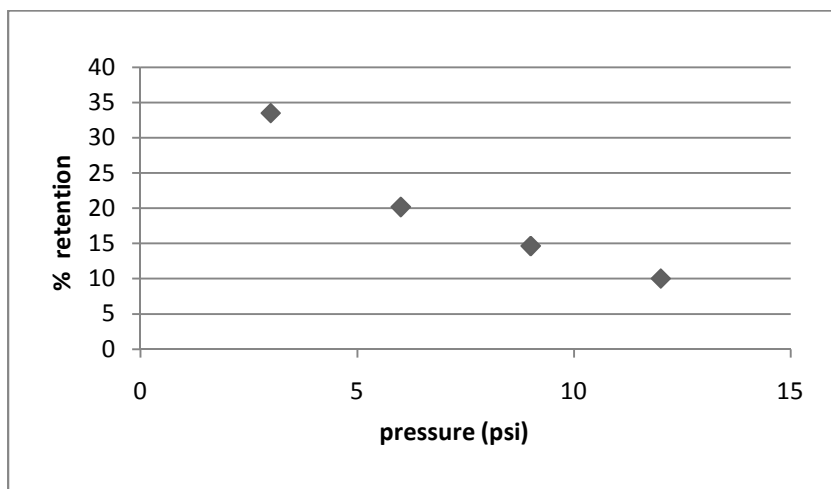
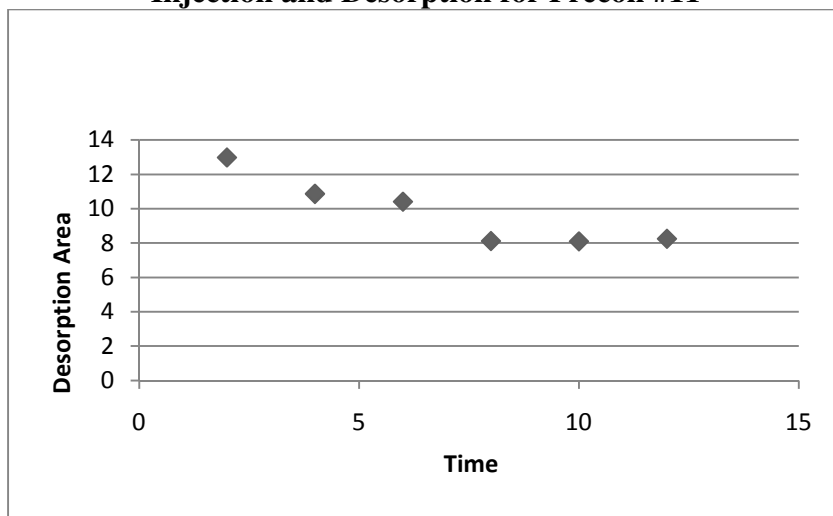


Figure 28: Desorption Peak Area of Hexane as a Function of Time between Injection and Desorption for Precon #11



Preconcentrator #R100: In order to calibrate flow to 1.0 mL/min through the setup when preconcentrator #R100 was installed, a system pressure of 3.1 psi was necessary. Blank heating runs were done before beginning an injection series and sometimes in the middle of a series.

Three adsorption/thermal desorption test runs conducted with 2.0 μ L vapor injections of hexane at a 10:1 split gave an average adsorbed mass of 204 ng, which was equivalent to a retention of approximately 28%. Four chlorobenzene runs of 2.0 μ L vapor injection volumes at a 10:1 split gave an average adsorbed mass of 476 ng, which corresponded to 51% analyte retention. Three adsorption/thermal desorption test runs conducted with 2.0 μ L vapor injections of 1,1,2,2-tetrachloroethane at a 10:1 split gave an average adsorbed mass of 1203 ng, which corresponded to a percentage of analyte retained of approximately 86%. Tables 19-21 summarize the adsorption data for the three compounds. Figure 29 shows a chromatogram for the two of the four chlorobenzene runs. The breakthrough peaks were wide with tailing, but the desorption peaks were sharp with a slight hitch-like irregularity in peak-shape. The 1,1,2,2-tetrachloroethane and hexane runs showed more irregular shapes for desorption peaks in which there were prominent double peaks. As with previous preconcentrators, the unusual peak shape made quantization of results less reliable.

Table 19: Hexane Adsorption/Desorption Results for Precon #R100

<u>split</u>	<u>breakthrough area</u>	<u>desorption area</u>	<u>total area</u>	<u>% retained</u>	<u>moles adsorbed</u>	<u>mass (ng) adsorbed</u>
10:1	851	272	1123	24.22084	2.01E-09	174
10:1	874	286	1160	24.65517	2.05E-09	177
10:1	459	265	724	36.60221	3.04E-09	262

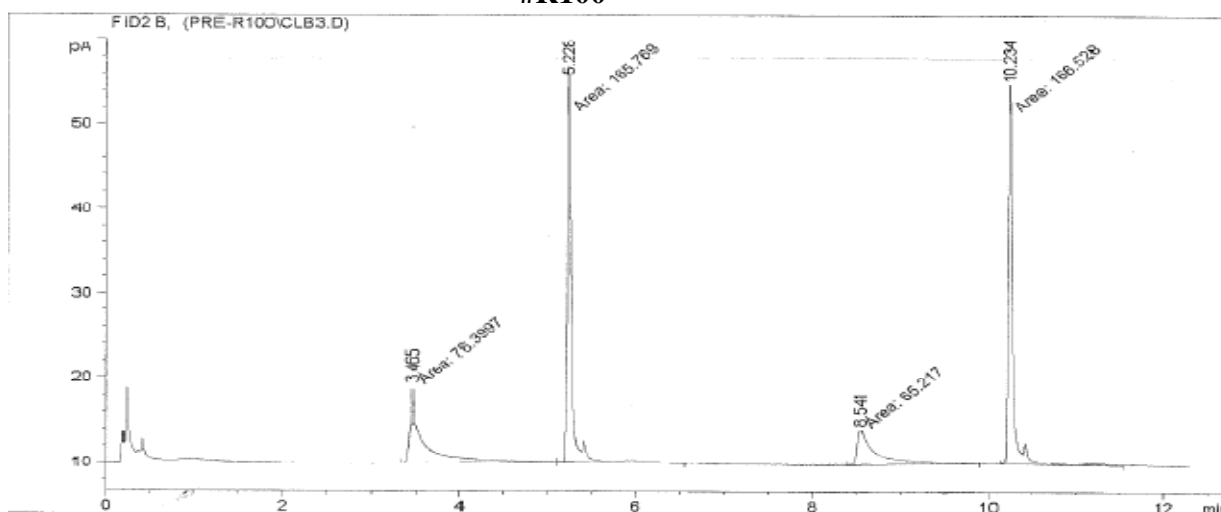
Table 20: Chlorobenzene Adsorption/Desorption Results for Precon #R100

<u>split</u>	<u>breakthrough area</u>	<u>desorption area</u>	<u>total area</u>	<u>% retained</u>	<u>moles adsorbed</u>	<u>mass (ng) adsorbed</u>
10:1	3419	1726	5145	33.5	2.79E-09	314
10:1	788	918	1706	53.8	4.47E-09	504
10:1	508	731	1239	59.0	4.91E-09	553
10:1	551	731	1282	57.0	4.74E-09	534

Table 21: 1,1,2,2-Tetrachloroethane Adsorption/Desorption Results for Precon #R100

<u>split</u>	<u>breakthrough area</u>	<u>desorption area</u>	<u>total area</u>	<u>% retained</u>	<u>moles adsorbed</u>	<u>mass (ng) adsorbed</u>
10:1	52.6	341	393.6	86.6	7.21E-09	1210
10:1	44.2	330.7	374.9	88.2	7.34E-09	1232
10:1	59.7	304.2	363.9	83.6	6.95E-09	1167

Figure 29: Chlorobenzene Adsorption/Desorption Runs 10:1 Split for Precon #R100



Preconcentrator#R200: In order to calibrate flow to 1.0 mL/min through the setup when preconcentrator #R200 was installed, a system pressure of 2.8 psi was necessary. Blank heating runs were done before beginning each series of runs.

Five chlorobenzene runs of 2.0 μ L vapor injection volumes at a 10:1 split gave an average adsorbed mass of 648 ng, which corresponded to 69% analyte retention. Five adsorption/thermal desorption test runs conducted with 2.0 μ L vapor injections of 1,1,2,2-tetrachloroethane at a 10:1 split gave an average adsorbed mass of 872 ng, which corresponded to a percentage of analyte retained of approximately 62%. These data are summarized in tables 22 and 23. Figure 30 shows a chromatogram for the chlorobenzene runs. The breakthrough peaks were moderately tailing, but the desorption peaks were sharp and narrow.

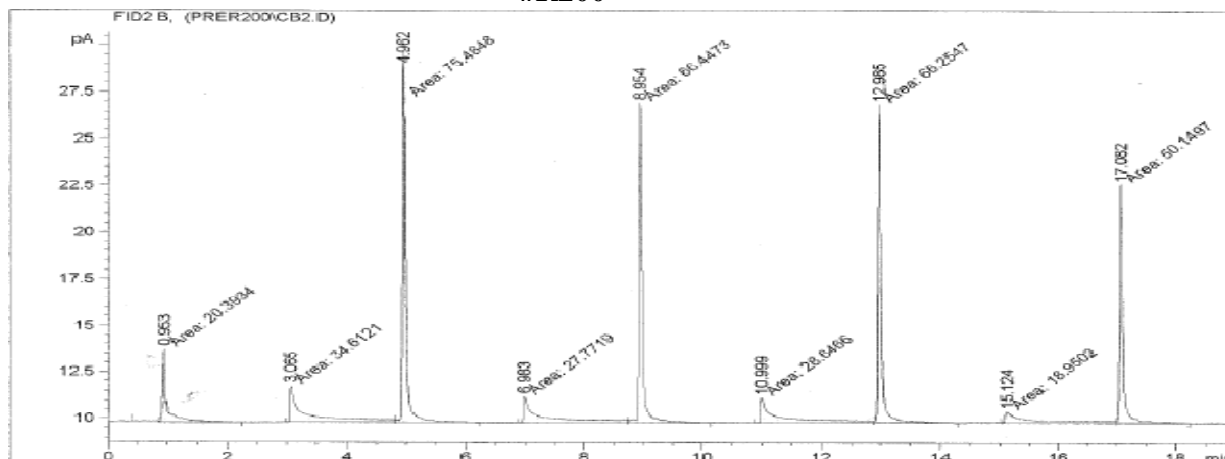
Table 22: Chlorobenzene Adsorption/Desorption Results for Precon #R200

<u>split</u>	<u>breakthrough area</u>	<u>desorption area</u>	<u>total area</u>	<u>% retained</u>	<u>moles adsorbed</u>	<u>mass (ng) adsorbed</u>
10:1	42.7	78.4	121.1	64.73988	5.39E-09	606
10:1	34.6	75.5	110.1	68.57402	5.70E-09	642
10:1	27.8	66.4	94.2	70.48832	5.86E-09	660
10:1	28.6	66.3	94.9	69.86301	5.81E-09	654
10:1	19	50.1	69.1	72.50362	6.03E-09	679

Table 23: 1,1,2,2-Tetrachloroethane Adsorption/Desorption Results for Precon #R200

<u>split</u>	<u>breakthrough area</u>	<u>desorption area</u>	<u>total area</u>	<u>% retained</u>	<u>moles adsorbed</u>	<u>mass (ng) adsorbed</u>
10:1	16	29.6	45.6	64.91228	5.40E-09	906
10:1	17.9	27.6	45.5	60.65934	5.05E-09	847
10:1	18.9	30.1	49	61.42857	5.11E-09	858
10:1	17.3	32	49.3	64.90872	5.40E-09	906
10:1	17.8	27.1	44.9	60.35635	5.02E-09	843

Figure 30: Chlorobenzene Adsorption/Desorption Runs, 10:1 split for Precon #R200



Comparison of Preconcentrators: The average masses of analytes adsorbed are shown comparatively in the bar graphs in Figures 31 and 32. All of the preconcentrators showed similar patterns of compound adsorption affinities where the capacity for 1,1,2,2-tetrachloroethane was greater than the capacity for chlorobenzene, which was in turn greater than the capacity for hexane. In the coated preconcentrators, the capacities for 1,1,2,2-tetrachloroethane and chlorobenzene were much greater than the capacity for hexane. The capacities tended to follow the expected order of decrease relative to conventional Tenax trap findings, probably due to the sorbent properties of Tenax.

Preconcentrator #11 appeared to trap larger amounts of 1,1,2,2-tetrachloroethane and chlorobenzene than all other preconcentrators tested. It also appeared to trap more hexane than all of the other surface-coated preconcentrators (#s 2, 5, 6, 8, 9). Perhaps this is due to the criss-cross geometric interior design which involved embedded micro-bars instead of square or circular posts. This may be related to flow direction/pathway and readily accessed surface area. Additionally, the peak

shapes for #11 were some of the most ideal among all of those obtained in preconcentrator testing.

The two web-coated preconcentrators, #s R100 and R200, had the next best trapping results. This is likely a function of the surface area, locations of adsorption sites, three-dimensional winding flow pathways through and around the webbing, and parabolic reflector design. Peaks from these preconcentrators were slightly noisier, but overall better than the average obtained peaks for the adsorption/thermal desorption runs in this study.

Missing data, lack of an uncoated control for every design, and compromised peak integrations all made comparison difficult.

Figure 31: Average masses of analytes retained by preconcentrators for adsorption/thermal desorption runs of 2.0 μ L injections at a 10:1 split flow

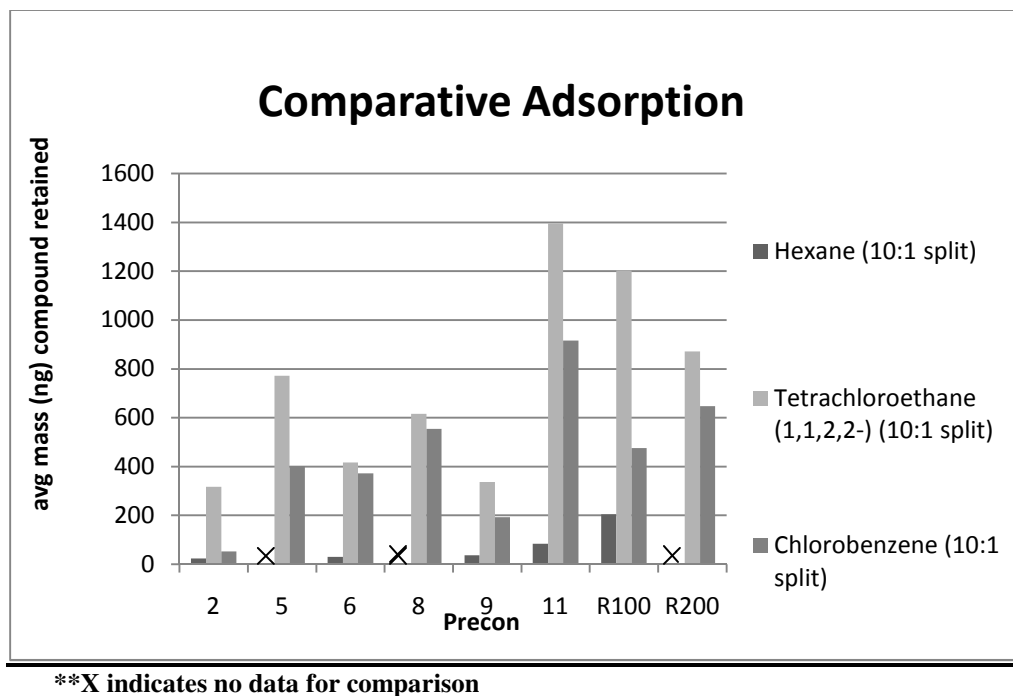
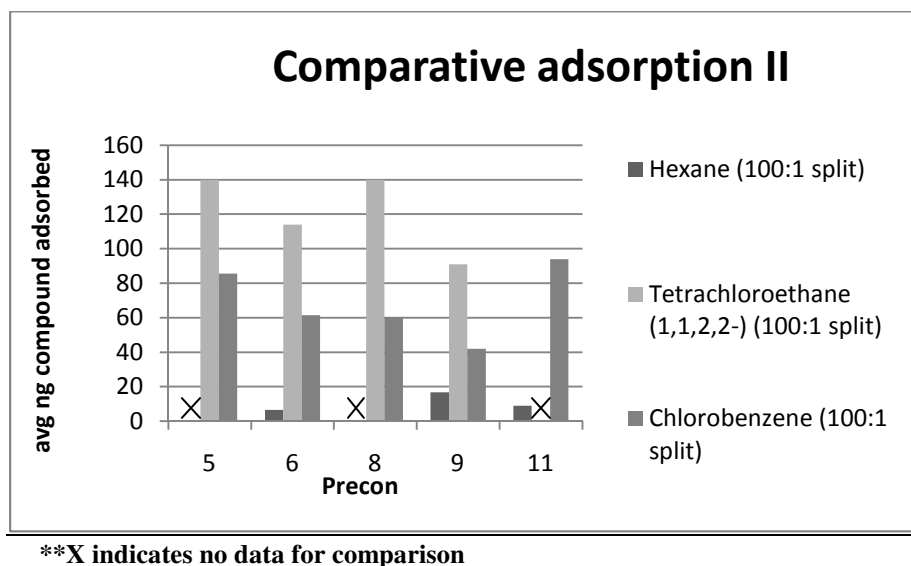


Figure 32: Average masses of analytes retained by preconcentrators for adsorption/thermal desorption runs of 2.0 μ L injections at a 100:1 split flow

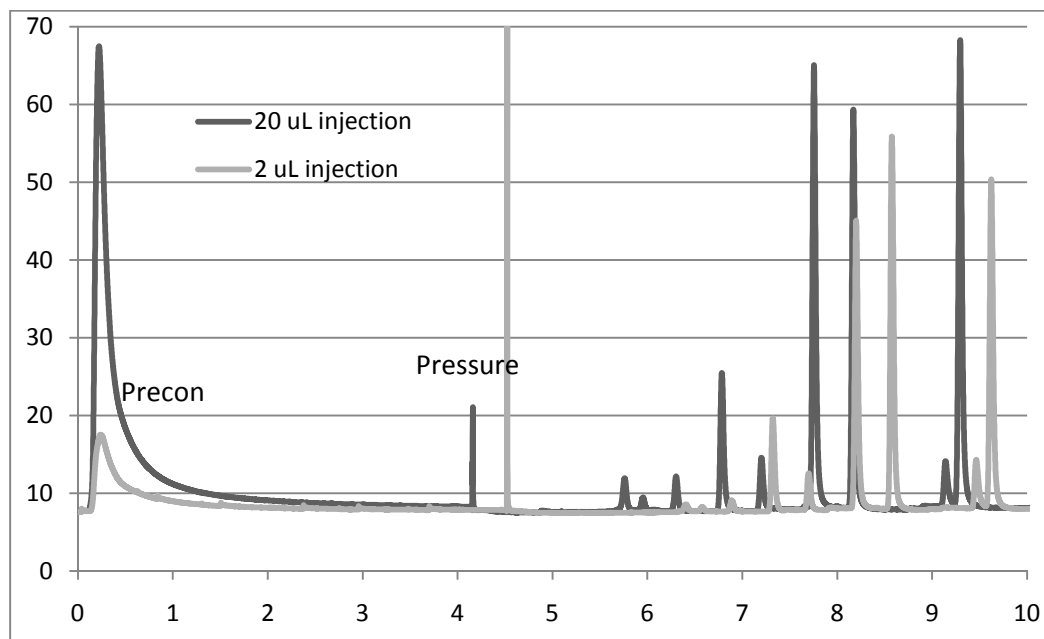


Preconcentrator-to-Column Coupling Experiment: The two chromatograms in Figure 33 show several resolved peaks from the 10-component VOC vapor mixture. The peak shapes and heights from the 2 μ L injection correspond to similar, relatively proportional peaks from the 20 μ L injection. As expected, the signals for the peaks from the 20 μ L injection were greater than those for the peaks of the 2 μ L injection. The two chromatograms were not time-normalized but can be aligned together due to their relative intensity patterns.

The spike following the breakthrough peak represents the pressure switch necessary to achieve effluent separations on the 15 m capillary column. Most of the ten compounds were resolved. Normalization and more testing are required for quantitative analysis, but from a preliminary perspective, this experiment can serve as a proof of concept to show that it is feasible to collect a mixture of analytes on a

MEMS-fabricated preconcentrator and then release the analytes via thermal desorption onto a column for effective separation and subsequent detection.

Figure 33: Preconcentrator-to-Column Chromatograms using Precon #R200



IV. Results and Discussion: Preliminary SPME Studies

Ten-Component VOC Mix Standard Runs on the GC-MS: Injections of 1.0 μL of the VOC mixes in pentane ranging in concentration from 0.01 ppm to 100 ppm were used to obtain sequential chromatograms and calibrate the detector response. The areas from these chromatograms were used to construct the graph in Figure 34. As expected, the signal for each compound increased linearly with concentration.

SPME Fiber Headspace Analysis of Spiked Water: Several SPME runs of varying concentrations gave peak separations with fluctuating areas. Eventually it was found that the rubber stopper used to cap the sample tube actually trapped some of the vapors being tested. The stopper was then switched to a PTFE cap, but due to instrumental problems and time constraints, no additional SPME runs were able to be conducted.

The chromatogram shown in Figure 35 shows three of the original runs made with the rubber stopper cap. All ten compound peaks were resolved. Peak identity was predicted based on elution being in order of increasing compound boiling point. This predicted elution order was confirmed with mass spectra for the individual peaks. See table 2 for compounds in order of elution along with their boiling points.

VOC solutions in methanol were used for water spiking to aid in solubilization of the VOC mix. The chromatograms of separate 40.0 mL spiked water samples with VOC concentrations of 10 ppb, 1 ppb, and 0.1 ppb, as represented in Figure 35, did show a decrease in signal with concentration.

Figure 34: Ten Component Mix Standard Calibration

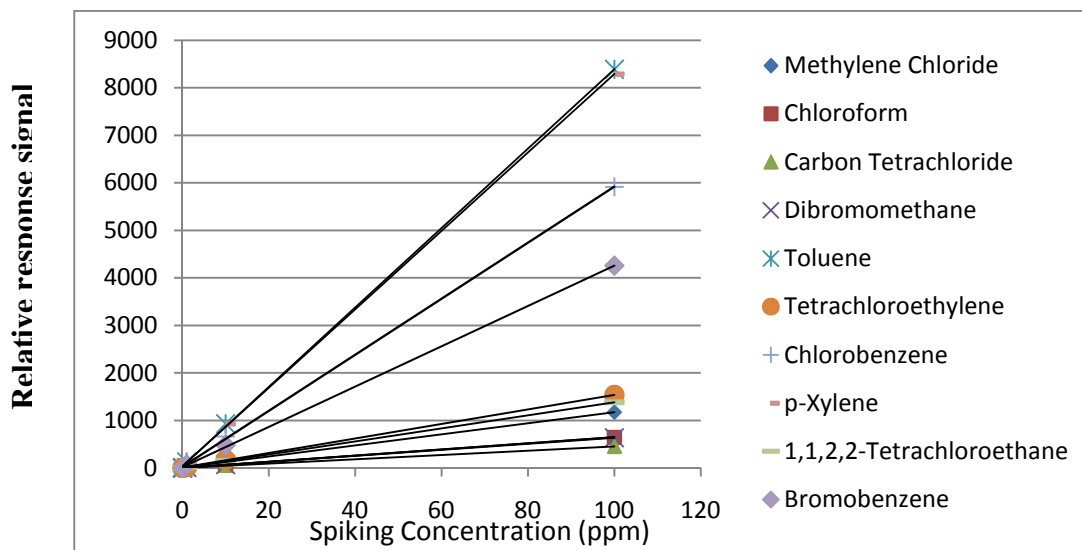
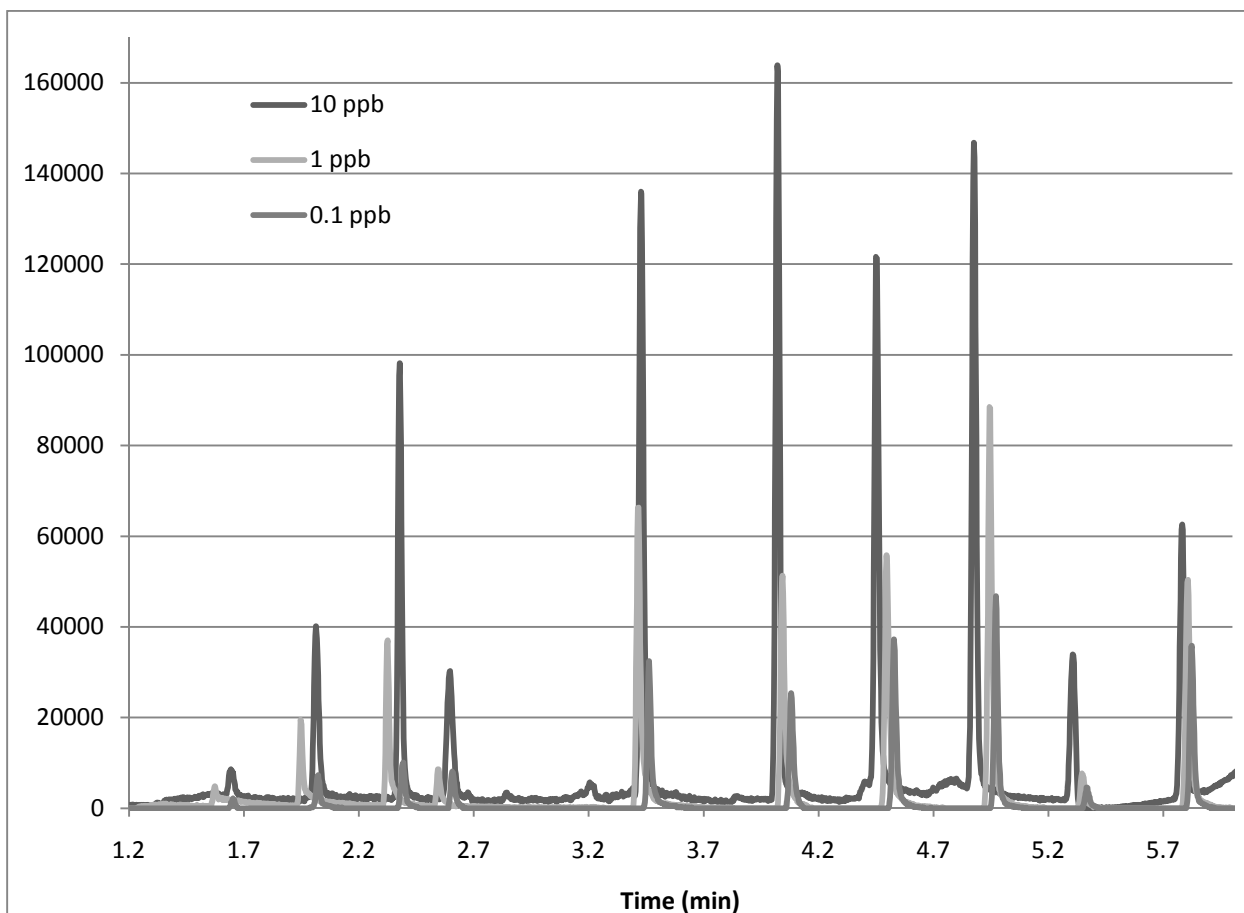


Figure 35: Preliminary SPME chromatograms



Since repeated trials were unable to be run, it cannot be determined whether or not this relationship might be linear. This experiment should be repeated with modifications to overcome procedural difficulties. Nevertheless, Tenax appears to be a viable adsorbent for SPME applications.

V. Conclusions and Future Work

The Tenax-coated preconcentrators and SPME fibers successfully adsorbed and thermally desorbed VOC vapors as expected. However, irregular peak shapes, experimental inconsistencies, and instrumental problems resulted in a lack of substantial quantitative data. Nothing concretely conclusive can be said about preconcentrator designs and fiber efficacy at this point, but this study suggests that the surface-coated criss-cross micro-bar designed preconcentrator and the two web-coated preconcentrators may be able to hold more analyte, and thus might be more useful than other designs in preconcentrator applications in gas chromatography.

Although methods for micropreconcentrator and SPME fiber evaluations were developed, time constraints prevented extensive testing of devices. Only one uncoated preconcentrator was evaluated in this experiment. In future work, it is suggested that there be an evaluation of at least one uncoated preconcentrator of each design for the sake of controlled comparison with coated preconcentrators. For the general sake of assessing reproducibility in fabrication, coating, setup, it is also recommended that there be evaluations of preconcentrators with identical designs. Perhaps at least one duplicate of every type of preconcentrator could be tested.

During preconcentrator testing, there were inconsistencies in the time between injection and desorption as well as the frequency of blank heating runs during a test series, a result of initial testing without a clear feel for what to expect. The normalization of these two factors would likely provide better repeatability and more reliable quantitative results. It is suggested that a time delay study such as the one developed in this project for preconcentrator #11, except that the study should be conducted for all compounds at all splits used instead of only for hexane at a 10:1 split. As for the blank heating runs, a series of at least three blank runs should be conducted before evaluation in order to check for background desorption signal or potential bleeding of the polymer coating or capillary seal. Moreover, there should be consistency in the frequency of blank heatings, and it is suggested that there be at least one blank heating in between each run in a series to ensure that all runs have similar starting conditions.

In addition, flow splits and volumes could be varied, but setup and parameters should be systematically repeated for each preconcentrator tested. A significant factor in calibration of flows is that the GC uses electronic flow control based on predescribed columns, thus split flows need to be verified for accurate accounting of the split ratios. For the preconcentrators in this study that always showed breakthrough, lower effective volumes of analyte could be used either by decreasing the injection volume or by altering the split ratio. An attempt should be made to reach a point where no breakthrough is observed because in applied analytical situations, it would be ideal for all analyte of interest to be trapped by the preconcentrator.

Future work with preconcentrators will involve on-chip resistive heaters and temperature sensors. In this project, the rapid heating panel could not be temperature-

controlled and only provided a pulse of heat to the chips. Engineering better control over the heating of preconcentrators, such as maintaining the high temperature for a fixed period of time, might yield more repeatability from run to run. Moreover, this kind of built-in heating system is what would ideally be used in actual micro-GC systems.

More preconcentrator-to-column testing should be conducted as well. If successful with conventional columns, perhaps coupling to micro-fabricated columns will follow. Eventually, some of the preconcentrator designs tested in this study might advance to testing in fully integrated micro-systems. There should be more isolated preconcentrator studies before this is done, though.

The SPME tests in this project were only preliminary studies. Much more investigation of the Tenax-coated fibers needs to take place before conclusions can be drawn about their efficacy. The primary objective of the SPME studies was to demonstrate linear adsorption over a broad concentration range and at ultra trace levels of VOCs. Perhaps this will be done in future studies. Some suggestions for the SPME work include careful timing of equilibration, even stirring, adding salt to drive vapors out of solution, and possibly heating to vaporize more semi-volatile compounds. In addition to headspace analyses, submerged fiber studies might also be attempted. This would involve dipping fibers in solution instead of just holding them in the headspace region. A new generation of Tenax coated fibers are currently being produced by the Agah group that have much more uniform coatings that should significantly enhance uniform equilibration of the adsorbent with analyte vapors and enhance reproducibility.

The preconcentrator studies might give insight into expectations for the SPME fiber studies since both utilize Tenax as a sorbent. One last suggestion might be to expand

the number of compounds used such that studies based on different variables such as polarity, volatility, and density could all be studied via groups of similar compounds. For example, the thermal stability of Tenax is significantly higher than any commercial adsorbent, thus less volatile analytes that cannot be effectively desorbed from commercial adsorbents may be better suited to Tenax SPME fibers. This may give more insight into the properties of Tenax as applied to micro-preconcentration and micro-extraction.

VI. References

- [1] W. C. Tian, H. K. L. Chan, C. J. Lu, S. W. Pang and E. T. Zellers, "Multiple-stage microfabricated preconcentrator focuser for micro gas chromatography system," *Journal of Microelectromechanical Systems* **14** (3), (2005) 498-507.
- [2] R. L. Grob, Modern Practice of Gas Chromatography, Fourth Edition (2004), Fourth Edition (eds R. L. Grob and E. F. Barry).
- [3] S. I. Ohira, K. Toda, "Micro Gas Analyzers for Environmental and Medical Applications," *Analytica Chimica Acta* **619** (2008) 143–156.
- [4] C. J. Lu, W. H. Steinecker, W. C. Tian, M. C. Oborny, J. M. Nichols, M. Agah, J. A. Potkay, H. K. L. Chan, J. Driscoll, R. D. Sacks, K. D. Wise, S. W. Pang, and E. T. Zellers, "First-generation hybrid MEMS gas chromatograph," *Lab on a Chip* **5**, (2005) 1123-1131.
- [5] S. Mitra, C. Feng, L. Zhang, W. Ho and G. McAllister, "Microtrap Interface for On-line Mass Spectrometric Monitoring of Air Emissions," *Journal of Mass Spectrometry* **34**, (1999) 478-485.
- [6] C. J. Lu and E. T. Zellers, "Multi-adsorbent preconcentrator/focusing module for portable-GC/microsensor-array analysis of complex vapor mixtures," *Analyst* **127**, (2002) 1061–1068.
- [7] A.M. Ruiz, I. Gracia, N. Sabate, P. Ivanov, A. Sanchez, M. Duch, M. Greboles, A. Moreno and C. Cane, "Membrane-suspended microgrid as a gas preconcentrator for chromatographic applications," *Sens. Actuators A* **135** (2007), 192–196.
- [8] M. Martin, M. Crain, K. Walsh, R.A. McGill, E. Houser, J. Stepnowski, S. Stepnowski, H.-D. Wu and S. Ross, "Microfabricated vapor preconcentrator for portable ion mobility spectroscopy," *Sens. Actuators B, Chem.* **126** (2007), 447–454.
- [9] M. Chai, J. Pawliszyn "Analysis of Environmental Air Samples by Solid-Phase Microextraction and Gas Chromatography/Ion Trap Mass Spectrometry" *Environ. Sci. Technol.* **29** (1995), 693-701.
- [10] M. Harper, "Sorbent trapping of volatile organic compounds from air," *Journal of Chromatography A*, **885** (1-2), (2000) 129-151.
- [11] A. Dabrowski, "Adsorption-from theory to practice," *Adv. Colloid Interface Sci.* **93** (2001) 135–224.
- [12] K.R. Solomon, X. Tang, S.R. Wilson, P. Zanis, A.F. Bais, "Changes in tropospheric

- composition and air quality due to stratospheric ozone depletion” *Photochem. Photobiol. Sci.* **2** (2003) 62–67.
- [13] C. M. Harris “GC to go,” *Anal. Chem.* **74**, 585A–589A (2002).
- [14] C. Saridara, R. Brukh, Z. Iqbal and, S. Mitra “Preconcentration of Volatile Organics on Self Assembled, Carbon Nanotubes in a Microtrap” *Analytical Chemistry* **77** (4),(2005) 1183-1187.
- [15] K. Bielicka-Daszkiewicz, A. Voelkel, “Theoretical and experimental methods of determination of the breakthrough volume of SPE sorbents,” *Talanta* **80** (2), (2009) 614-621.
- [16] O. B. Egorov, M.J. O'Hara, J.W. Grate, “Equilibration-Based Preconcentrating Minicolumn Sensors for Trace Level Monitoring of Radionuclides and Metal Ions in Water without Consumable Reagents” *Anal. Chem.* **78**, (2006) 5480–5490.
- [17] W.A. Groves, E.T. Zellers, G.C. Frye, “Analyzing organic vapors in exhaled breath using a surface acoustic wave sensor array with preconcentration: Selection and characterization of the preconcentrator adsorbent,” *Analytica Chimica Acta* **371**, (2-3), (1998) 131-143.
- [18] C. Grote, J. Pawliszyn, “Solid-Phase Microextraction for the Analysis of Human Breath,” *Anal. Chem.* **69** (1997), 587-596.
- [19] P. Popp, C. Bauer, L. Wennrich, “Application of Stir-Bar Sorptive Extraction in Combination with Column Liquid Chromatography for the Determination of Polycyclic Aromatic Hydrocarbons in Water Samples.” *Analytica Chimica Acta*, **2001**, 436, 1–9.
- [20] B. Alfeeli, H. Vereb, A. Dietrich, M. Agah, “Low pressure drop micro preconcentrators with cobweb Tenax-TA film for analysis of human breath,” MEMS 2011, Cancun, Mexico, January 23-27, 2011.
- [21] SIS Inc., Tenax TA Adsorbent Resin Physical Properties, <<http://www.sisweb.com/index/referenc/tenaxta.htm>> (2011).